Title: Derivation of functional early gestation decidual natural killer cell subtypes from induced pluripotent stem cells

Author list: Virginia Chu Cheung[1,2,3], Jennifer Jaimez[1,2,3], Carly DaCosta[1,2,3], Harneet Arora[1,2,3], Christine Caron[1,3], Jaroslav Slamecka[1,2,3], Manuel Fierro[2,5], Morgan Meads[1,2,3], Kathleen Fisch[3,4], Robert E. Morey[1,2,3], Luisjesus S. Cruz[2,5], Devika Pant[1,2,3], Dan S. Kaufman[2,5], Mariko Horii[1,2,3], Jack D. Bui[1,3,*], Mana M. Parast[1,2,3,*]

[1] Department of Pathology, School of Medicine, University of California San Diego, La Jolla, CA,92093, USA.

[2]Sanford Consortium for Regenerative Medicine, University of California San Diego, La Jolla, CA,92093, USA.

[3]Center for Perinatal Discovery, University of California San Diego, La Jolla, CA, 92093, USA.

[4]Department of Obstetrics, Gynecology, and Reproductive Sciences, School of Medicine, University of California San Diego, La Jolla, CA, 92093, USA.

[5]Department of Medicine, School of Medicine, University of California San Diego, La Jolla, CA, 92093, USA.

*Correspondence: mparast@health.ucsd.edu, jbui@health.ucsd.edu

Disclaimers: V.C.C., J.J., C.D., H.A., C.C., J.S., M.F., M.M., K.F., R.E.M., L.S.C., D.P., M.H., J.D.B, and M.M.P declare no competing interests. D.S.K. is a co-founder and advisor to Shoreline Biosciences and has an equity interest in the company. D.S.K. also consults Therabest and RedC Bio for which he receives income and/or equity. Studies in this work are not related to the work of those companies. The terms of these arrangements have been reviewed and approved by the University of California, San Diego, in accordance with its conflict-of-interest policies.

Abstract:

Abnormal decidual natural killer cell (dNK) function is linked to pregnancy complications occurring in both early and late gestation, including recurrent pregnancy loss, preeclampsia, and preterm birth. Exploration of dNK heterogeneity as it relates to function is an active area of research; however, most of this work has focused on early gestation. Using flow cytometric and transcriptomic single-cell definitions of dNK subtypes, we characterized dNK heterogeneity in term dNK within both chorioamniotic membranes and basal plate. We also applied aptamer-based secretome profiling to first trimester and term dNK, and found dNK-specific proteins – VEGF and PLGF – to be reduced at term. We further determined that, compared to first trimester dNK, term dNK have reduced cytoxicity against target cells. Finally, we applied this knowledge to establish a protocol for differentiation of induced pluripotent stem cells (iPSC) into functional dNK. We found that treatment with TGFβ enriched for dNK2 subtype, while inducing dNK markers, CD9 and CD103. We evaluated function using cytokine and degranulation assays, aptamer-based secretome profiling, and cytotoxicity assays. We found that iPSC-dNK are functionally most similar to primary dNK. Further, TGFβ iPSC-dNK had reduced GM-CSF in response to PMA/I and increased secretion of VEGF and other first trimester-specific proteins – supportive of a shift towards an early gestation, dNK2-dominant, phenotype. We conclude that changes in dNK function across gestation reflect shifts in dNK subtypes that can be reproducibly derived from iPSC, providing a new method for modeling dNK and laying the foundation for cell-based therapeutics for reproductive disease.

Significance Statement:

Alterations in maternal decidual natural killer cells (dNK) are associated with pregnancy complications – from recurrent pregnancy loss to preeclampsia and preterm birth. We found dNK from different regions of the term placenta to be distinct from peripheral blood NK and early

26 gestation dNK, based on gene and surface marker expression, subtype composition, secretome,
27 and cytotoxicity. We report a novel, reproducible protocol to generate dNK resembling the most
28 abundant dNK subtype in early gestation from induced pluripotent stem cells. Our study lays the
29 foundation for *in vitro* modeling of the maternal-fetal interface and therapeutic development for
30 reproductive disease.
31

32 **Introduction:**

33 A successful pregnancy requires maternal tolerance of the semi-allogeneic fetal-derived
34 placenta.[1] Prior to fertilization and embryo implantation, the uterine lining undergoes
35 decidualization, a morphologic and functional transformation, leading to a tissue poised for both
36 tolerance of fetal-derived antigens, and recognition and clearance of potential pathogens.[1,2] This
37 process involves infiltration with a vast array of maternal leukocytes, including natural killer (NK)
38 cells.[3] Decidual NK cells (dNK) are a type of tissue resident NK cell (trNK) found in the uterine
39 lining. dNK cells function to support implantation and promote angiogenesis by crosstalk with
40 maternal decidualized endometrial stromal fibroblasts (dESF) and fetal-derived extravillous
41 trophoblasts (EVT) in the placenta.[4,5] As gestation progresses, the maternal decidua contributes
42 to the basal plate (BP, also the decidua basalis) and chorioamniotic membranes (CAM, also the
43 decidua parietalis). dNK at the BP regulate EVT invasion and establish maternal blood flow to the
44 feto-placental unit.[5] Meanwhile, CAM functions as a protective barrier surrounding the fetus
45 throughout much of gestation. Abnormal dNK function has been associated with multiple
46 pregnancy complications including recurrent spontaneous pregnancy loss, preeclampsia, as well
47 as inflammation-induced spontaneous preterm birth.[6-9]

48 dNK have cell surface marker expression and function distinct from peripheral blood NK
49 cells (PB-NK). dNK in nonpregnant and first trimester decidua are $CD56^{bright}CD16^{-}$, and co-
50 express CD9, unlike $CD56^{dim}CD16^{+}CD9^{-}$ PB-NK.[10,11] In the NK-92 cell line, acquisition of CD9

51 results in increased production of proangiogenic IL-8, reduced production of proinflammatory
52 TNFα and IFNγ, and reduced cytotoxicity against target cells.[12] However, dNK at the maternal-
53 fetal interface are not the same throughout gestation. Inhibitory Killer Cell Immunoglobulin-Like
54 Receptors KIR2DL1 and KIR2DL2/3 are reduced in both BP- and CAM-dNK cells at term
55 compared to first trimester dNK.[13,14] At baseline, dNK and PB-NK express cytolytic molecules
56 (PFN, GZMB, GNLY); however, PB-NK have higher PFN and GZMB than dNK and first trimester
57 dNK (but not term dNK) have higher GNLY and 9kD GNLY.[13] Unstimulated, first trimester dNK,
58 but not PB-NK, secrete proangiogenic cytokines and growth factors (IL-6, VEGF, PLGF).[15,16]
59 These data are supportive of a role for dNK in vascular remodeling in early gestation, however,
60 the function of unstimulated term dNK have never been evaluated in this capacity.

61 Primary dNK have reduced cytotoxicity relative to PB-NK; however, this function is
62 context-dependent and regulated by the decidual niche. *In vitro* first trimester dNK demonstrate
63 reduced lysis of target cells in comparison to PB-NK, but first trimester dNK with high IL-15 will
64 lyse target cells more than PB-NK.[17] In addition, first trimester dNK have been shown to lyse K562
65 and primary trophoblast target cells similar to PB-NK, but this is diminished in the presence of
66 decidual macrophages or TGFβ.[18] While term dNK degranulate in response to phorbol- 12-
67 myristate-13-acetate and ionomycin (PMA/I) stimulation and K562 at levels similar to PB-NK, term
68 dNK have different expression of cytolytic proteins relative to both PB-NK and first trimester
69 dNK.[13] Thus, it remains unclear if term dNK have the capacity to kill target cells.

70 Nevertheless, it is known that PB-NK, first trimester dNK, and term dNK cells have distinct
71 activation responses. PB-NK induce higher levels of CD107a and cytokines (TNFα, IFNγ, GM-
72 CSF), compared to first trimester dNK, in response to PMA/I stimulation.[13,15] Given the same
73 stimulation, term dNK (BP and CAM) respond with high CD107a, similar to PB-NK, yet have a
74 modest pro-inflammatory cytokine response (TNFα, IFNγ), similar to first trimester dNK. Although
75 certain activation receptors (*CD69*, *NKp80*, *NKp44*) are expressed at the RNA level in CAM-dNK,

76 but not in BP-dNK, functional and protein expression differences have not yet been identified.[13,19-
77 21] dNK function and receptor expression are distinct between first trimester and term (including
78 between BP and CAM), however, the basis for this functional change remains unclear.

79 Recent single-cell analyses have pointed to first trimester dNK's transcriptional and functional
80 heterogeneity, identifying 4 subtypes, dNK1, dNK2, dNK3 and dNKp.[22-24] dNK1 express CD39
81 (*ENTPD1*), an inhibitory receptor expressed by trNK found in tonsil, liver, and first trimester
82 decidua, CD39 knocked out mice have increased NK cell numbers and NK effector functions.[11,25]
83 dNK2 and dNK3 express CD18 (*ITGB2*), an integrin that enhances NK cell cytotoxicity.[26] dNK3
84 also express CD103 (*ITGAE*), a tissue residency marker for lung NK cells, as well as T cells in
85 multiple tissue types.[27,28] Expression of CD103 by dNK is associated with higher cytokine (GM-
86 CSF, XCL1) and CD107a expression, after PMA/I stimulation.[23] Following stimulation, dNK3 have
87 the highest GM-CSF expression followed by dNK2, then dNK1 with low levels similar to PB-
88 NK.[23,24] Importantly, dNK subtypes differentially express receptors and ligands (*CCL5*, *LILRB1*,
89 *CSF1*) used for interaction with placental EVT and other cell types– suggesting distinct roles in
90 placentation.[22] However, it is not known how changes in these subtypes relate to functional
91 changes throughout gestation at different locations within the maternal-placental interface.

92 Due to lack of access to decidual tissues in an ongoing pregnancy, studies rely on model
93 systems. Mouse placentation is distinct from human at structural, cellular, and molecular levels.[29]
94 Importantly, human and mouse placental cells at the maternal-placental interface do not have the
95 same expression of key receptor/ligand pairs involved in dNK crosstalk.[30] Similarly, PB-NK and
96 term dNK significantly differ from their first trimester counterparts, both in their immunophenotype
97 and functional capacity.[3,13, 31-33] While attempts have been made to generate dNK from PB-NK,
98 primary NK cells are difficult to reliably expand in culture – limiting their capacity for mechanistic
99 studies.[34,35] This necessitates novel models to study human dNK and their integral interactions
100 with maternal and placental cells.

101 Over the past two decades, generation of patient-specific induced pluripotent stem cells
102 (iPSC) from somatic cells has revolutionized the modeling of numerous human diseases.[36] We
103 and others have shown that preeclampsia (PE)-associated cellular abnormalities can be modeled
104 using iPSC. This includes abnormal differentiation and function of trophoblast, derived from iPSC,
105 obtained by reprogramming cells from PE-affected placentas,[37-39] as well as abnormal function of
106 endothelial cells, derived from iPSC, obtained by reprogramming peripheral blood mononuclear
107 cells (PBMCs) from patients with PE.[40] Currently, there are protocols to routinely generate mature,
108 cytotoxic $CD56^+CD16^+$ NK cells from iPSC. These iPSC-NK transcriptionally resemble umbilical
109 cord and PB-NK and kill tumor cells *in vitro* and *in vivo.*[41-43] Several clinical trials have now
110 demonstrated that engineered iPSC-NK are safe and effective in treatment of refractory
111 malignancies.[36,44] However, no protocol exists to generate dNK from iPSC.
112 Studies in mice and human suggest one mechanism of dNK emergence to be through PB-NK
113 infiltration and exposure to the decidual niche,[45,46] where the oxygen tension throughout gestation
114 is 2-8% O_2.[47] In fact, IL-15 and exposure to low oxygen tension induce a dNK-like phenotype in
115 PB-NK.[34,35] Trophoblast-derived SDF-1 (*CXCL12*) stimulate PB-NK migration into decidua, and
116 PB-NK coculture with EVT has been shown to promote conversion to a dNK-like phenotype.[45,48]
117 Furthermore, treatment of PB-NK with TGFβ1, a growth factor secreted by maternal dESF and
118 placental EVT, in combination with hypoxia, promote a dNK-like phenotype, including induction
119 of CD9, reduced cytotoxicity, and increased VEGF secretion.[27,35] In this study, we characterize
120 dNK heterogeneity and function at first trimester and different regions of the term placenta, and
121 apply this improved understanding of dNK gene expression, surface protein and cytokine
122 expression, protein secretion, and cytotoxicity, to establish a differentiation protocol to derive
123 functional dNK from iPSC.
124
125 **Materials and Methods**
126 For detailed protocols, see **Supplementary Materials and Methods.**

127 **Patient recruitment and tissue collection**

128 Human decidual and blood tissue samples were collected under UCSD IRB-approved protocols
129 (IRB #181917 and 172111); all patients gave informed consent.

130 **hPSC**:

131 Human pluripotent stem cell (hPSC) experiments were performed under protocol #171648,
132 approved by the UCSD IRB and Embryonic Stem Cell Research Oversight Committee. Human
133 embryonic stem cell (hESC) WA09/H9 and 3 iPSC lines (established as a part of the biorepository
134 of the Center for Perinatal Discovery) were used for differentiation.

135

136 **Results:**

137 Defining primary dNK subtypes by scRNA-seq and flow cytometry across gestation

138 We set out to identify first trimester dNK subtypes (dNK1, dNK2, dNK3, and dNKp) in term
139 decidua.[22,23] We reanalyzed previously-published scRNA-seq datasets from blood and first
140 trimester decidua (Vento-Tormo, 2018) as well as term placental and decidual tissues (Pique-
141 Regi, 2019).[22,49] We utilized all cells in the Vento-Tormo dataset, and verified NK cells by
142 expression of NK-associated genes (**Supplementary Figure 1A, B**). We extracted all the NK
143 cells (peripheral blood, PB-NK; and decidua, dNK) (**Figure 1A**), to use as a reference. We
144 compared gene expression between these reference NK cells, in the absence of non-NK cell
145 types, to identify new NK cell subtype-specific marker genes for dNK1, dNK2, dNK3, dNKp, PB-
146 NK $CD16^+$, and PB-NK $CD16^-$ (**Figure 1A**, **Supplementary Figure 1C**, **Table 1, Supplementary**
147 **File 1)**.

148 In the Pique-Regi dataset, three compartments in the term placenta (BP; CAM; and
149 placental villus, PV) were annotated using sample-associated meta data (**Supplementary Figure**
150 **1D,E**). We verified NK cells by expression of NK-associated genes (**Supplementary Figure 1F**).
151 We extracted all NK cells from the Pique-Regi dataset and mapped them to our reference NK

152 cells.[22] All dNK subtypes found in first trimester could be identified at term, with dNK2 making up
153 the majority of the dNK in first trimester decidua (45%) and term CAM (57%) while dNK3 make
154 up the majority in term BP (71%) (**Figure 1B**). Meanwhile, dNK1 made up only 6% of BP-dNK
155 and 5% of CAM-dNK, while $\leq$0.1% of all term dNK mapped to dNKp (**Figure 1B**). We applied our
156 new NK cell subtype- specific markers (**Supplementary Figure 1C**) to the term NK dataset and
157 found an abundance of cells expressing dNK3 marker, *CCL5*, with smaller populations of cells
158 expressing the dNK2 marker, *ZNF683* (also known as HOBIT), and dNK1 marker, *SPINK2*, and
159 only rare cells expressing the dNKp marker *MKI67* (**Supplementary Figure 1C,G,H, Table 1**).
160 We found there were more dNK2 marker, *ZNF683*$^+$ NK cells in CAM and more dNK3 marker,
161 *CCL5*$^+$ NK cells in BP (**Supplementary Figure 1I**). This agrees with the reference mapping
162 results, which identified more dNK2 in CAM and more dNK3 in BP (**Figure 1B**). The Pique-Regi
163 dataset contains cells from placentas delivered at term, with and without labor, as well as those
164 delivered preterm with labor.[49] Across all three labor groups, dNK3 were increased in both
165 compartments relative to first trimester, with dNK3 dominant in BP, and dNK2 dominant in CAM
166 (**Supplementary Figure 1J.**).

167 We next characterized dNK in early first trimester decidua and term placenta, the latter
168 including decidua from both BP and CAM, by flow cytometry (**Figure 1C**). We confirmed that dNK
169 are CD45$^+$CD56^{bright}CD16$^-$ and comprise 40-70% of CD45$^+$ cells in first trimester and term
170 decidual tissues (**Figure 1D**). dNK-associated CD9 and trNK-associated CD69 were expressed
171 by a large proportion of dNK throughout gestation (**Figure 1E**).[12,20] CD9$^+$ dNK was significantly
172 reduced, 1.4-fold in term BP (71.9% mean) and 1.2-fold in CAM (87.0% mean), compared to first
173 trimester. Quantification by Median Fluorescent Intensity (MFI) showed a significant increase in
174 CD69 in term dNK in both compartments (**Figure 1E**).

175 We next evaluated dNK subtype-associated markers. dNK1 marker CD39 (*ENTPD1*) was
176 expressed by an average of 74.9% of dNK in first trimester but was reduced over 8-fold (9.0%
177 mean) in term BP and almost 3-fold (26.5% mean) in term CAM (**Figure 1F**). [22,24] Similarly,

178 KIR2DL1, a marker of both dNK1 and dNK2, was expressed by an average of 67.2% of first
179 trimester dNK, but only 17.5% and 6.4% of term BP and CAM, respectively (**Figure 1F**). [22,23] In
180 contrast, CD18 (*ITGB2*), a marker of both dNK2 and dNK3 was ~5-fold higher in term BP (93.0%
181 mean) and term CAM (80.0% mean), compared to first trimester (17.6% mean) (**Figure 1G**). dNK3
182 marker CD103 (*ITGAE*) was expressed by an average of ~55%, ~39%, and 42% of the dNK in
183 early gestation decidua, term BP, and term CAM, respectively (**Figure 1G**). [22,23] However, like
184 CD18, CD103 MFI was upregulated at term, increased by ~11-fold and 13.5-fold in term BP and
185 CAM, respectively (**Figure 1G**). This is consistent with scRNA-seq results, which showed that
186 dNK1 are more abundant in first trimester decidua, while dNK3 are relatively more abundant at
187 term, in both BP and CAM. Flow cytometry of dNK2-associated KIR2DL1 and CD18 were
188 incongruous with each other; however, scRNA-seq analyses using marker gene and
189 unsupervised (reference mapping) analyses pointed to dNK2 as the most abundant subtype in
190 first trimester and term CAM.

191 Term BP- and CAM-dNK have greater expression of activating receptors and
192 degranulation response than first trimester dNK.[13] When first trimester dNK is sub-stratified by
193 subtype, dNK3 has the highest degranulation and cytokine expression (effector response),
194 followed by dNK2, and then dNK1 upon PMA/I stimulation.[23,24] In agreement with the literature,
195 we found markers associated with decreased effector function (CD9, CD39 and KIR2DL1) to be
196 higher in first trimester dNK, while activating receptors (CD69, CD18, and CD103) were increased
197 at term, in both BP and CAM (**Figure 1E - G**). Interestingly, CD39, KIR2DL1, and CD18 were
198 dramatically changed between first trimester and term. CD9, CD69, and CD103 were maintained
199 by a more constant proportion of dNK, although levels of CD69 and CD103 were higher at term,
200 compared to first trimester. Together, these data suggest that functional changes in dNK across
201 gestation may be driven by a shift in dNK subtypes, with decreased dNK1 (low effector function,
202 high levels of inhibitory molecules) and increased dNK3 (high effector function, high levels of

203 activating molecules) as gestation progresses toward term. Additionally, we identify the proportion
204 of dNK2 and CD9$^+$ dNK to be similar between first trimester and term CAM.

205 iPSC-NK acquire dNK markers in response to TGFβ treatment

206 We next set out to establish an *in vitro* model of dNK, by differentiation of pluripotent stem cells
207 (both embryonic and induced PSC). We used a protocol, modified from Zhu et al., 2019,[50] to
208 differentiate the hESC line H9/WA09, and 3 different iPSC lines, generated and validated in our
209 own lab (**Supplementary Figure 2A-E**), into iPSC-NK. At the start of this protocol (**Figure 2A**),
210 hematopoietic stem/progenitor cells were generated from highly pure, SSEA4$^+$ hPSC (**Figure 2B,**
211 **C**), using a spin embryoid body (EBs) method. EBs containing CD34$^+$ cells (**Figure 2B, D**) were
212 plated for NK differentiation. After 28 days, round cells emerged in suspension. An average of
213 87.3% of these cells were CD45$^+$, of which 78.2% were also CD56$^+$ (**Figure 2B, E**). To enrich for
214 NK, these cells were collected for expansion. Instead of coculture with artificial antigen presenting
215 cells as previously published,[50] we cultured the cells in a commercially available media (see
216 **Methods**) supplemented with IL-2 and IL-15 for this expansion phase. After 2 weeks of
217 expansion, an average of 87.8% of CD45$^+$ cells were also CD56$^+$, with 15.6% CD56$^+$CD16$^+$, and
218 72.2% CD56$^+$CD16$^-$ (**Figure 2B, F**).

219 We hypothesized conditions mimicking the decidual niche would promote a dNK
220 phenotype. We reclustered the NK cells from the Vento-Tormo dataset broadly into two groups:
221 dNK (comprised of dNK1, dNK2, dNK3, and dNKp), or PB-NK (comprised of NK CD16$^+$ and NK
222 CD16$^-$) (**Supplementary Figure 3A**) and compared the two to identify an enrichment in TGFβ
223 signaling and hypoxia pathways in dNK (**Supplementary Figure 3B**). Additionally, TGFβ and
224 CXCL12 have been shown to promote dNK-like phenotype when applied to PB-NK.[34,35,45] We
225 tested TGFβ and CXCL12 under 5% or 21% O_2, during the expansion phase of our protocol. We
226 found TGFβ, but not CXCL12 or 5% O_2, slightly increased the proportion of CD56$^+$CD16$^-$,
227 decreased CD18, and significantly increased dNK markers CD9 (2-fold) and CD103 (~90-fold)

228 (**Figure 2G, H, I, Supplementary Figure 3C, D**). TGFβ had no effect on CD69 and dNK-
229 associated CD49a (**Figure 2J,K**).

230 Together, these data show that we can derive NK cells from hPSC, and that TGFβ pushes
231 the cells further toward a dNK phenotype.

232 <u>iPSC-NK are transcriptionally similar to dNK, not PB-NK, and TGFβ induces the dNK2 phenotype</u>

233 We further characterized our iPSC-NK, with and without TGFβ, using scRNA-seq (**Figure**
234 **3A**). We found that iPSC-NK expressed dNK marker genes (*NCAM1*, *ITGA1*, *CD69*) and no
235 *FCGR3A* (PB-NK-associated CD16) (**Figure 3B**). We again used the full Vento-Tormo dataset as
236 a reference, with NK cells subclustered broadly as dNK (comprised of dNK1, dNK2, dNK3, and
237 dNKp), or PB-NK (comprised of NK $CD16^+$ and NK $CD16^-$) (**Supplementary Figure 3A**).[22] We
238 found 94% of iPSC-NK cells mapped to dNK (**Figure 3C,D**). iPSC-NK also expressed dNK-
239 (*SPINK2*, *ZNF683*, *CCL5*), but not PB-NK- (*SELL*, *SPON2*) associated markers (**Supplementary**
240 **Figure 4A**). These data indicate that the iPSC-NK, regardless of TGFβ treatment, transcriptionally
241 resemble dNK, not PB-NK; henceforth, we will refer to our cells as iPSC-dNK, no TGFβ treatment
242 as NT iPSC-dNK, and TGFβ treated cells as TGFβ iPSC-dNK.

243 We next investigated iPSC-dNK heterogeneity using unsupervised and supervised
244 analyses. Unsupervised clustering of iPSC-dNK resulted in 11 clusters, with clusters 0-7
245 representing the majority (99%) of cells (**Figure 3E; Supplementary Figure 4B**). Hierarchical
246 clustering grouped clusters 0, 1, and 6 into one clade, comprised of TGFβ iPSC-dNK (**Figure 3F**),
247 expressing TGFβ-inducible genes, *JUN* and *SMAD7* (**Supplementary Figure 4C**). Clusters 2, 3,
248 and 5 were grouped into another clade, comprised of no treatment (NT) iPSC-dNK (**Figure 3F**).
249 Clusters 4 and 7 were grouped into a third clade, comprised of G2M and S phase cells expressing
250 proliferation genes (*MKI67*, *PCNA*). (**Supplementary Figure 4D,E**). Finally, clusters 8, 9, and 10,
251 comprising a small minority (0.5%) of cells, mapped primarily to non-NK populations (**Figure 3C**).

252 We identified marker genes for each cluster and continued with gene enrichment analysis
253 of each of the major clades (**Supplementary File 2**). Both the NT and TGFβ clades were enriched
254 for many pathways involved in NK cell function such as Protein Secretion, IL6 JAK/STAT3
255 signaling, and IL-2/STAT5 signaling (**Supplementary File 3**, **Figure 3G**).[51-53] We also found an
256 enrichment for dNK-specific signaling pathways, Interferon Alpha and Gamma Response, and
257 TGF-beta signaling (**Figure 3G**, **Supplementary Figure 3B**). Interestingly, all three of these dNK-
258 specific pathways were more significantly enriched within the TGFβ clade (**Figure 3G,** triangle).
259 Additionally, we found that there was an enrichment of genes involved in both "TGF-beta
260 signaling" and "PI3K/AKT pathway" in the TGFβ clade, suggesting that our TGFβ treatment was
261 acting via both canonical and non-canonical pathways (**Supplementary File 3**).[54] As expected,
262 DEGs in the proliferating clade were enriched for cell cycle control (**Supplementary File 3**).
263 Notably, there was enrichment for "Lymphoid cells of the Placenta" in both NT and TGFβ clade
264 enriched DEGs (**Supplementary Tables 1-3**), consistent with the dNK identity predicted by
265 reference mapping. However, pathway analysis identified differential activation of immune
266 signaling pathways between NT and TGFβ clades suggestive of more nuanced differences
267 between the iPSC-dNK. iPSC-dNK showed dNK-associated gene expression that was further
268 enriched by TGFβ.

269 To compare the heterogeneity of the iPSC-dNK to that of dNK *in vivo,* we extracted the
270 dNK subclusters (dNK1, dNK2, dNK3, dNKp) from Vento-Tormo et al.,[22] to use as a reference for
271 iPSC-dNK (**Supplementary Figure 4F**). We found the majority of cells (42%) in the NT clade
272 mapped to dNK3, with the next largest population of cells (32%) mapping to dNK2, followed by
273 dNK1 (22%), while the TGFβ clade found 86% of cells mapping to dNK2, 12% to dNK1, and only
274 1% to dNK3 (**Figure 3H,I, Supplementary Figure 4G**). Further, the iPSC-dNK expressed dNK,
275 but not PB-NK, marker genes, and showed an enrichment of dNK2 marker gene *ZNF683* within
276 the TGFβ clade (**Figure 3J, Supplementary Figure 4A**).

277 In summary, scRNA-seq analysis confirmed the dNK identity of iPSC-dNK. We identified
278 heterogeneity within the iPSC-dNK, representing relevant dNK subtypes, finding that TGFβ further
279 enriches for dNK signaling pathways and alters the proportion of dNK subtypes in favor of dNK2.

280 iPSC-dNK functionally resemble dNK

281 With the dNK identity of the iPSC-dNK established, we set out to analyze their function.
282 dNK from early and late gestation express cytolytic proteins.[13] We found that NT and TGFβ iPSC-
283 dNK expressed *GNLY*, *PRF1*, and *GZMB* (**Supplementary Figure 5A**) by scRNA-seq. We also
284 found protein expression, albeit at low levels, of PFN (encoded by *PRF1*) and the first trimester
285 dNK-specific 9kD GNLY isoform in both NT and TGFβ iPSC-dNK (**Supplementary Figure 5B-**
286 **C**).[13]

287 First trimester dNK, not PB-NK, secrete IL-6, VEGF, and PLGF in the absence of
288 stimulation.[15,16] However, it is not known if term or iPSC-dNK share this function. We applied
289 aptamer-based proteomic profiling, using the SomaScan Assay 7K panel (See **Methods**) to
290 conditioned media from purified NK cells from peripheral blood, first trimester decidua, and term
291 BP and CAM, and compared them to those of NT iPSC-dNK and TGFβ iPSC-dNK (**Figure 4A**).
292 We found 4,938 proteins secreted by primary cells at levels above media-only control, of which
293 1,456 were found in first trimester, BP, or CAM dNK, but not PB-NK (**Figure 4B**); of these 1,456
294 proteins, 570 were shared by all 3 primary dNK (**Supplementary Figure 6**). We found iPSC-dNK
295 secreted proteins had substantial overlap with those from primary dNK, and not PB-NK (**Figure**
296 **4C**). TGFβ induced secretion of a markedly higher number of dNK-specific proteins, compared to
297 NT iPSC-dNK (217 in TGFβ iPSC-dNK, vs. only 28 in NT iPSC-dNK) (**Figure 4C**).

298 Transcriptionally, TGFβ iPSC-dNK were enriched for dNK2, the most represented subtype
299 in first trimester dNK (**Figure 1B**). We therefore asked if the secretory function of TGFβ iPSC-
300 dNK reflected that of first trimester dNK. Of the 253 first trimester dNK-specific proteins
301 (**Supplementary Figure 6A**), 127 were identified in TGFβ-treated iPSC-dNK secretome while

302 only 74 were identified in NT iPSC-dNK (**Figure 4D**). We saw the same enrichment when we
303 considered all 3,683 proteins secreted by first trimester dNK, with 3,231 also secreted by TGFβ
304 iPSC-dNK (**Supplementary Figure 6B**). In agreement with prior literature, we found levels of IL-
305 6, VEGF, and PLGF were higher by 2.5-fold, 2.7-fold, or 2.1-fold, respectively, in first trimester
306 dNK, compared to PB-NK (**Figure 4E**). We also report, for the first time, that high IL-6 and PLGF
307 are in fact specific to first trimester dNK, as their levels are lower in BP- and CAM-dNK
308 secretomes, which are more similar to that of PB-NK (**Figure 4E**). Interestingly, we found TGFβ
309 iPSC-dNK secrete higher levels of VEGF and PLGF, comparable to first trimester dNK (**Figure**
310 **4E**).

311 In comparison to first trimester dNK, primary term dNK and PB-NK have similarly higher
312 degranulation (CD107a) in response to PMA/I stimulation. However, compared to PB-NK,
313 stimulated first trimester and term dNK have lower production of cytokines (IFNγ, TNFα).[13] GM-
314 CSF, on the other hand, has a reciprocal response, with higher induction in first trimester dNK
315 than PB-NK.[23] Within first trimester dNK subtypes, in comparison to dNK2, dNK3 responded with
316 higher levels of CD107a, GM-CSF, and IFNγ.[23,24] We found iPSC-dNK to be responsive to PMA/I
317 stimulation, inducing CD107a, IFNγ, TNFα, and GM-CSF, with decreased production of TNFα
318 and GM-CSF in TGFβ-treated cells (**Figure 5A-D**).

319 Finally, we evaluated the cytotoxicity of NT and TGFβ iPSC-dNK relative to term CAM-
320 and BP-dNK, first trimester dNK, PB-NK, and NK-92 cells, against JEG3 choriocarcinoma target
321 cells, at 1:1, 2:1, and 5:1 effector-target (E:T) ratios (**Figure 6A**). In alignment with the current
322 literature, we found that first trimester dNK trend towards inducing apoptosis in target cells at
323 reduced levels relative to NK-92 and PB-NK (**Figure 6B-C**). Interestingly we found that increasing
324 numbers of BP- or CAM-dNK do not induce increased apoptosis in target cells (**Figure 6B-C**).
325 Finally, we found that NT and TGFβ iPSC-dNK were able to kill target cells (**Figure 6B-C**),
326 demonstrating functional maturity, similar to primary first trimester dNK and PB-NK.

327 In summary, we found that, overall iPSC-dNK are functionally most similar to primary dNK,
328 and that TGFβ iPSC-dNK have increased secretion of first trimester dNK-specific proteins and
329 reduced stimulation response, supportive of a first trimester dNK (dNK2-dominant) phenotype.
330

331 **Discussion:**

332 dNK are a key cell type during pregnancy, playing vital roles from implantation in early gestation,
333 to continued regulation of EVT function at the basal plate (BP), and regulation of membrane
334 rupture in chorioamniotic membranes (CAM) during labor. These various functions may be
335 mediated by different dNK subtypes.[22-24] We found dNK subtype compositions between first
336 trimester decidua and term BP and CAM reflected this change in function. We also present novel
337 analysis of NK cell function in our study, and report the secretome of first trimester dNK, term BP-
338 and CAM-dNK, and PB-NK, as well as the first characterization of term BP- and CAM-dNK
339 cytotoxicity. We used these primary cell data, in combination with published literature to develop
340 a rigorous dNK scorecard, against which to benchmark newly developed models (**Figure 7**). To
341 this end, we report a robust, reproducible, and tunable protocol for induction of functional dNK
342 from iPSC, as measured by surface markers, transcriptome, secretome, and functional activation.
343 In agreement with previous literature, we found term dNK show greater expression of
344 activating receptors, compared to first trimester dNK. We also identified a high proportion of high-
345 effector function dNK3 at term, increased from first trimester, suggesting this increase in dNK3 is
346 mediating the increased activating receptors, decreased inhibitory receptors, and increased
347 PMA/I response observed in term dNK. However, while we found BP-dNK to have the greatest
348 proportion of dNK3 based on scRNA-seq analysis, percent positivity for CD103 (a dNK3 marker)
349 was not significantly increased, relative to first trimester or term-CAM dNK, suggesting
350 discordance between transcriptomic and proteomic subtype definitions. Previous studies have
351 found that term dNK show decreased expression of some cytolytic molecules (GNLY, 9kD GNLY),
352 but not others (PFN, GZMB), relative to first trimester dNK. In comparison with first trimester dNK,

353 term dNK degranulation is higher in response to PMA/I and K562 target cells, but lower in
354 response to HCMV-infected decidual stromal cells.[13] As such, it is unclear whether term dNK
355 possess the capacity to kill a target cell and how this capacity compares to first trimester dNK and
356 PB-NK. We found that term BP- and CAM-dNK did not induce apoptosis of JEG3 cells with
357 increasing E:T ratios, while first trimester dNK did, albeit at levels below PB-NK and NK-92. Our
358 study provides new information on how dNK are functionally changed throughout gestation and
359 decidual locations reflecting the dynamic nature of the maternal-placental interface while
360 highlighting the need for more comprehensive definitions for dNK subtypes.

361 dNK heterogeneity is an emerging area of study. While variegated expression of cell
362 surface markers by dNK have long been observed, the field has only recently begun defining dNK
363 subtypes as scRNA-seq technologies and analysis tools have improved. As such, transcriptional
364 definitions are most universally accepted, while cell surface markers and functional outputs
365 associated with dNK1, dNK2, and dNK3 are still being defined. While this limits the conclusions
366 we can draw from our own data, our study begins to bring the transcriptomic, flow cytometric, and
367 functional definitions of dNK together, using primary and iPSC-derived dNK. Importantly, we
368 expect our iPSC-derived model to accelerate research in this space.

369 Studies of term dNK have shown no differences in protein expression or function based
370 on localization in BP vs. CAM. However, term dNK from the two compartments do show gene
371 expression differences.[13] Single-cell analyses have pointed to a relative increase in dNK in CAM,
372 but not BP, in placentas of patients with preterm labor.[49,55] Further, labor-associated differential
373 interactions have been identified in full term BP-dNK and CAM-dNK.[56] Our reanalysis of these
374 data identified similar differences between BP- and CAM-dNK.[49] Notably, we found that ~50% of
375 the dNK in CAM are dNK2, similar to first trimester, while the dNK2 is reduced (to 23%) in BP.
376 dNK3 dominance over dNK2 in BP and dNK2 over dNK3 in CAM was consistent between term
377 with and without labor (see **Supplementary Figure 1J**). Interestingly, we observed increased
378 dNK3 in CAM in placentas with labor (term or preterm) but decreased dNK3 in BP of placentas

379 from patients with preterm labor. Due to the small sample size (n=3 per labor group), we conclude
380 that these observations warrant follow up studies on dNK subtypes in both BP and CAM in the
381 context of labor, particularly preterm labor.

382 We found the proportion of dNK2 (scRNA-seq) and $CD9^{+}CD56^{bright}CD16^{-}$ dNK (flow
383 cytometry) were similar between first trimester decidua and term CAM; meanwhile, term BP
384 showed decreased dNK2 based on scRNA-seq and decreased $CD9^{+}CD56^{bright}CD16^{-}$ by flow
385 cytometry. While the frequencies of $CD9^{+}$ dNK (~90%) and dNK2 (~50%) are not the same within
386 a single tissue, these data suggest CD9 could be used, in combination with other markers, to
387 define dNK2. We add further support for this relationship using our newly-developed
388 differentiation protocol for iPSC-dNK. TGFβ treatment resulted in selection against dNK3, in favor
389 of dNK2, based on transcriptome, increased CD9 by flow cytometry, as well as reduced GM-CSF
390 secretion by PMA/I stimluation. These data from both primary and iPSC-dNK suggest that CD9,
391 in combination with other markers, may be useful to identify a dNK2 transcriptional phenotype;
392 however, additional experiments are needed to validate this concept.

393 Our study is the first application of untargeted aptamer-based proteomic profiling of
394 secretome from primary NK cells, including first trimester and term dNK and PB-NK. We applied
395 this method to iPSC-dNK and functionally compared them to primary dNK. Of the more than 4,000
396 proteins identified in the secretomes of primary NK cells, we found approximately 1/3 to be dNK-
397 specific. We also found similarities in dNK across gestation – with significant overlap between first
398 trimester and term BP dNK - as well gestational age-related changes, such as reduced secretion
399 of proangiogenic proteins at term (**Supplementary Figure 6A**). TGFβ treatment is typically shown
400 to suppress NK cell activation and function.[34,35,57] Notably, however, TGFβ treatment of PB-NK
401 alone does not induce VEGF secretion.[58] We found that TGFβ iPSC-dNK secrete VEGF at levels
402 significantly higher than PB-NK (**Figure 4E**), supportive of TGFβ promoting differentiation to dNK.
403 Interestingly, we observed no enrichment of *VEGF* transcript by any dNK subtype in first trimester

404 decidua (data not shown); however, VEGF levels were similar in TGFβ iPSC-dNK and first
405 trimester dNK secretomes, suggesting this could be a functional signature of dNK2. However,
406 follow up studies are required to validate this interpretation.

407 Historically, iPSC-derived cells have been found to be immature and not fully functional.[36]
408 However, this is not the case for iPSC-derived NK cells, as they have been used *in vivo* and in
409 the clinic.[43,44,59] While short term exposure to TGFβ is associated NK cell suppression,[43] long-term
410 exposure to TGFβ during NK activation, known as "TGFβ imprinting," is associated with
411 heightened cytokine secretion, degranulation, and cytotoxicity.[60] We find that NT and TGFβ iPSC-
412 dNK are functionally mature, as shown by their secretion of cytokines and angiogenic proteins,
413 as well as their cytotoxicity against target cells. Further, TGFβ iPSC-dNK had increased secretion
414 of angiogenic proteins and a trend towards higher induction of apoptosis in target cells, perhaps
415 consistent with the dNK2 phenotype, which reportedly show moderate cytokine induction and
416 degranulation in response to PMA/I stimulation;[23,24] however cytolytic protein expression and
417 cytotoxicity of dNK subtypes have not been evaluated. Overall, our findings emphasize the need
418 for integrated transcriptomic and functional definitions of dNK subsets.

419 A major limitation of our model system is that our iPSC-dNK are derived and cultured in
420 the absence of *in vivo* spatial, endocrine, and cellular cues. Previous scRNA-seq analyses have
421 identified potential interaction partners between dNK and other decidual cell type, such as EVT
422 and dESF.[22] However, due to limitations in access and cell yield, it is difficult to use primary cells
423 to develop more complex multi-cell type 3-dimensional models to study such *in vivo* cues and
424 validate these hypothesized interactions. We have previously generated maternal dESF and
425 placental EVT from iPSC and here established a protocol for differentiation of dNK from iPSC.[38,61]
426 Our iPSC-based models can overcome limitations, such as cell yield which introduces allogenic
427 incompatibilities, in particular between maternal dESF and dNK, in cocultures. Further, these
428 models offer technical advantages for mechanistic studies using gene editing.[43,44] In our NT and

429 TGFβ iPSC-dNK, we observed expression of *CCL5* and *XCL1*, known partners of *CCR1* and
430 *XCR1*, respectively, expressed by EVT, macrophages, and dendritic cells.[22] Furthermore, we can
431 induce specific receptors and ligands by modulating expansion phase media composition.
432 Specifically, NT iPSC-dNK showed high *XCL2* and *KLRB1*, partners for *XCR1* and *CLEC2D*,
433 respectively, expressed by EVT, dESF, and dendritic cells; conversely, TGFβ iPSC-dNK showed
434 high *CXCR4* and *CSF1*, partners for *CXCL12* and *CSFR1*, respectively, expressed by dESF and
435 macrophages.[22] The abundant cell yield and the ability to control receptor expression without
436 antibody purification - and thus interference - will enable studies of specific interactions affecting
437 placentation and pregnancy outcomes between dNK and other cell types.

438 A second limitation of this study is that we cannot rule out transcriptional similarity of our
439 iPSC-dNK to tissue-resident (tr)-NK of other tissues. Indeed, this would be an interesting line of
440 investigation, as dNK share expression of CD69 and CD103 with trNK cells, found in the
441 lungs.[28,63,64] scRNA-seq of human blood, tonsils, lung, and intestinal mucosa clustered NK cells
442 into 4 broad categories: $CD56^{Bright}$ and $CD56^{Dim}$, both which can be found in tissues and blood,
443 and $PRDM1^{+}$ ILC1 and $ZNF683^{+}$ NK, found only in tissue. [63,64] The authors compared these NK
444 subtypes to dNK and found dNK1 was most similar to intestinal intraepithelial $PRDM1^{+}$ ILC1, while
445 dNK2 and dNK3 most closely resembled $ZNF683^{+}$ NK found in lung and tonsil. We identified
446 *ZNF683* as a dNK2 marker which can be enriched for in iPSC-dNK by TGFβ. These data suggest
447 that follow up analyses of TGFβ iPSC-dNK may find resemblance to lung and tonsil $ZNF683^{+}$ NK,
448 broadening the applications of our protocol.

449 Just as iPSC-NK are being developed as cellular therapies for cancer treatment, it is
450 paramount that we also develop these technologies into therapeutics for reproductive conditions.
451 Our protocol offers a first step toward development of such therapeutics, and hopefully, the
452 prevention of adverse pregnancy outcomes.
453

454 **Resource Availability**

455

456 **Materials availability**

457 This study did not generate new unique reagents. Requests for further information, reagents, and
458 human pluripotent stem cell lines used in this study should be directed and will be fulfilled by the
459 Lead contact, Mana Parast (mparast@health.ucsd.edu).

460 **Data and code availability**

461 • Single-cell RNA-seq data are deposited at GEO and publicly available as of the date of
462 publication. Accession numbers will be listed in the key resources table (GSE302146).
463 • This paper does not report original code. The final code used for data processing and
464 analysis will be deposited at Zenodo and made publicly available as of the date of
465 publication. DOIs are listed in the key resources table.
466 • Any additional information required to reanalyze the data reported in this paper is available
467 from the corresponding author upon request.

468

469 **Acknowledgements and Funding:**

470 The authors are grateful to all patients who donated tissues for this research. This work was
471 funded by the National Institutes of Health (NIH) (R01-HD102639 to M.M.P. and J.D.B.; R00-
472 HD091452 to M.H.), NIH/NCATS 2UL1TR001442-08 (CTSA), as well as faculty-generated
473 discretionary funds. V.C.C. was supported by F32-HD108944 and T32-HD007203 to the
474 University of California, San Diego. M.H. was also supported by the UCSD Academic Senate
475 grant RG106839. J.D.B. was also supported by The Hartwell Foundation. C.D. was supported by
476 the California Institute for Regenerative Medicine Bridges Grant EDUC2-08376 awarded to San
477 Diego State University. J.J. supported by the California Institute for Regenerative Medicine
478 Bridges Grant EDU-1261 awarded to California State University San Marcos. This publication
479 includes data generated at the UC San Diego IGM Genomics Center utilizing an Illumina NovaSeq

480 6000 that was purchased with funding from a National Institutes of Health SIG grant (#S10
481 OD026929). Computational analysis was performed on the Extreme Science and Engineering
482 Discovery Environment (XSEDE) Expanse at SDSC, which is supported by National Science
483 Foundation grant number ACI-1548562 (allocation ID: BIO220095). Graphical abstract and
484 schematics in Figure 1, Figure 2, Figure 4, Figure 6, Figure 7, and Supplementary Figure 2 were
485 created in BioRender. Cheung, V. (2026) https://BioRender.com/pxhkijv

486 **Figure Legends:**

487 **Figure 1. Term dNK cells show enrichment in activated dNK subtypes**. **A)** UMAP showing
488 NK cell reference from Vento-Tormo, 2018[22] containing dNK and PB-NK subtypes. **B)** Pie charts
489 showing dNK subtype composition in decidua from first trimester, term basal plate (BP), and term
490 chorioamniotic membrane (CAM), as identified by reference mapping of term scRNA-seq data
491 from Pique-Regi et al., 2019[49] to **(A)** (data from Pique-Regi reanalyzed with permission). **C)**
492 Schematic of primary cell samples used for flow cytometric analysis. **D-G)** Representative FACS
493 plots and quantification of NK cell markers (CD56 and CD16), in first trimester decidua, term BP,
494 and term CAM after gating on Live $Lin^{-}CD45^{+}$ **(D)**, as well as dNK markers (CD9 and CD69) **(E)**,
495 inhibitory receptors (CD39 and KIR2DL1) **(F)**, and activating receptors (CD18 and CD103) **(G)**
496 after gating on Live $Lin^{-}CD45^{+}CD56^{bright}CD16^{-}$ cells. For **D** through **G**, data are represented as
497 mean +/- standard error, n = 8 individual patients (4 first trimester donors and 4 term placenta
498 donors; BP and CAM were dissected and processed separately from the same term placentas).
499 Statistical analysis was performed using ordinary one-way ANOVA with multiple comparisons
500 using GraphPad Prism; *p<0.05, **p<0.01, ***p<0.001, ****p<0.0001.

501 Alt text: UMAP showing NK cell heterogeneity. Pie charts showing dNK subtype composition
502 across gestation. Histograms and bar graph quantification of cell surface marker expression on
503 first trimester, Term BP, and Term CAM dNK cells.

504 **Figure 2. TGFβ supplementation increases dNK cell marker expression in iPSC-NK**. **A)**
505 Schematic of the entire differentiation protocol. **B)** Representative phase images of cells

506 throughout the differentiation process. **C-E)** Representative FACS plot and quantification of
507 expression over isotype control. Pluripotency marker SSEA4 staining in iPSC, before starting the
508 differentiation **(C)**, hematopoietic stem progenitor cell (HSPC) marker CD34 staining after EB
509 formation, before plating for NK cell differentiation **(D)**, and immune cell marker CD45 and NK cell
510 marker CD56 staining after NK cell differentiation, before plating for expansion **(E)**. **F)**
511 Representative FACS plot of CD56 and PB-NK marker CD16 co-staining after at least 2 weeks
512 of expansion in IL-2 and IL-15. $CD56^+CD16^-$ and $CD56^+CD16^+$ populations are quantified. **G)**
513 Quantification of $CD45^+CD56^+CD16^-$ population in No Treatment (NT, no TGFβ) and TGFβ
514 treatment conditions. **H-K)** Quantification of flow cytometric staining of dNK associated markers,
515 CD9 **(H)**, CD103 **(I)**, CD69 **(J)**, and CD49a **(K)**, in iPSC-NK at the end of the expansion phase.
516 For **C** through **K**, data are represented as mean +/- standard error. For **C** through **F**, n = 4 PSC
517 lines; H9 hESC line and MB3140, MB3144, LD2809 iPSC lines. For **G** through **K,** n = 11
518 independent experiments using MB3140, MB3144, LD2809 iPSC lines, Statistical analysis was
519 performed using Ordinary one-way ANOVA with multiple comparisons using GraphPad Prism;
520 *p<0.05, **p<0.01, ***p<0.001, ****p<0.0001.
521 Alt text: Schematic of iPSC differentiation protocol. Bright phase images of cells throughout
522 differentiation. Histograms and bar graphs quantifying expression of markers during key phases
523 of differentiation. Scatter plot and bar graphs showing dNK-like and PB-NK-like cells. Bar graphs
524 showing increased dNK marker expression in iPSC-NK after TGFbeta treatment.
525 **Figure 3. iPSC-NK cells transcriptionally resemble dNK cells, with TGFβ promoting a dNK2**
526 **phenotype**. 2 iPSC lines (MB3140 and MB3144 lines) differentiated with and without TGFβ were
527 subjected to scRNA-seq, resulting in 4 samples with a total of 33,830 cells after filtering for
528 analysis (MB3140_NT: 9147 cells; MB3144_NT: 6628 cells; MB3144_TGFβ: 9152 cells;
529 MB3140_TGFβ: 10,031 cells). **A)** UMAP showing no treatment (NT, no TGFβ) and TGFβ iPSC-
530 NK cells derived from MB3140 and MB3144 iPSC lines. Unsupervised clustering resulted in

separation by treatment group with TGFβ-treated cells on the left and NT on the right. **B)** FeaturePlots showing expression of dNK marker genes (*NKG7*, *NCAM1*, *CD69*) and absence of PB-NK marker gene *FCGR3A*, which encodes CD16. **C)** UMAP showing predicted identities for iPSC-NK, using all cells from Vento-Tormo et al., 2018[22] with dNK (comprised of dNK1, dNK2, dNK3, and dNKp) and PB-NK (comprised of NK CD16+ and NK CD16-) as reference. **D)** Pie chart quantification of data in **(C)**. **E)** UMAP showing clustering of iPSC-dNK at 0.4 resolution. **F)** Dendrogram showing phylogenetic analysis of aggregate gene expression of iPSC-dNK clusters; TGFβ clade in blue, NT clade in red, Proliferative clade in green. **G)** Quantification of pathways significantly enriched in both NT and TGFβ clades using MSigDB Hallmark 2020 pathway analysis. There are two values per pathway, one each from NT clade-enriched DEGs (circles) and TGFβ clade-enriched DEGs (triangles). **H)** UMAP showing all predicted identities for iPSC-dNK cells, using the dNK cell subtypes (dNK1, dNK2, dNK3, dNKp) from Vento-Tormo, 2018[22] as reference. **I)** Pie chart quantification of data in **(H)**. **J)** *ZNF683*, dNK2 marker gene, has significantly higher expression in TGFβ iPSC-dNK in comparison to NT iPSC-dNK. Statistical analysis was performed by Wilcox Rank Sum test using R. ****$p < 0.0001$

Alt text: UMAPs showing NK cell marker expression by iPSC-NK. UMAPs and Pie chart showing dNK cell identify of 94% of iPSC-NK. UMAP and dendrogram showing clustering of iPSC-dNK by treatment group. Graph showing gene enrichment in dNK-associated pathways by iPSC-dNK, with further enrichment upon TGFbeta treatment. UMAP and pie chart showing iPSC-dNK resemble all dNK subtypes with increased proportion of dNK2 upon TGFbeta treatment. Violin Plot showing higher expression of dNK2-marker gene ZNF683 in TGFbeta iPSC-dNK

Figure 4. iPSC-dNK secrete proteins similar to primary dNK. A) Schematic of experimental design for aptamer-based proteomic profiling. **B)** Venn Diagram showing 2,875 proteins identified in conditioned media of first trimester, term BP-, and term CAM-dNK, as well as PB-NK; 1,456 proteins found only in primary dNK media (dNK-specific); and 607 proteins found only in PB-NK

556 media (PB-NK-specific). **C)** Venn Diagram showing overlap of proteins identified in secretome of
557 NT and TGFβ iPSC-dNK with dNK-specific (1,456) and PB-NK-specific (607) proteins;
558 significantly higher overlap was noted with the dNK-specific proteins. **D)** Venn Diagram showing
559 overlap of proteins identified in secretome of NT vs. TGFβ iPSC-dNK with first trimester dNK-
560 specific (253) proteins; significantly more overlap was noted with TGFβ iPSC-dNK proteins. **E)**
561 Box plots showing median expression as well as individual $\log_{10}$RFU values for each sample.
562 Proteins known to be enriched in dNK (over PB-NK) are shown: IL-6 (seq.2573.20), VEGF
563 (seq.2597.8), and PLGF (seq.2330.2). Term BP n= 3, Term CAM n=2, First Trimester decidua n
564 =3, NT iPSC-dNK n = 3, TGFβ iPSC-dNK n=3, PB-NK n=3. Dunn's test for multiple comparisons,
565 using R, is shown; *p<0.05, **p<0.01.
566 Alt text: Schematic illustrating all NK cells analyzed by aptamer-based proteomic profiling. Venn
567 diagrams showing primary dNK secrete more proteins than PB-NK. Venn diagram showing iPSC-
568 dNK secreted more dNK-specific proteins than PB-NK-specific proteins. Venn diagram showing
569 TGFbeta iPSC-dNK express more first trimester dNK specific proteins than NT iPSC-dNK. Box
570 and whisker plots showing higher levels of IL-6, VEGF, and PLGF proteins in first trimester dNK
571 and TGFbeta iPSC-dNK.
572 **Figure 5. iPSC-dNK response to stimulation is modulated by TGFβ.** Representative FACS
573 plots for **A)** CD107a **B)** TNFα **C)** GM-CSF, and **D)** IFNγ of NT and TGFβ iPSC-dNK in the
574 presence or absence (unstim) of PMA/I treatment. Quantification of stimulation markers **E)**
575 CD107a **F)** TNFα **G)** GM-CSF, and **H)** IFNγ, as a percent of expression of dNK, as measured by
576 flow cytometry. Statistical testing was performed on PMA/I – unstim of n=4 independent
577 experiments are iPSC-dNK derived from MB3140 and MB3144 iPSC lines. Data in **E** through **H**
578 are represented as mean +/- standard error, by paired t-test using GraphPad Prism; *p<0.05.

579 Alt text: Histograms and bar graph quantification showing iPSC-dNK increase CD107a,
580 TNFalpha, GM-CSF, and IFNgamma in response to PMA/I stimulation. Statistical analysis shown
581 on bar graphs show decreased TNFalpha and GM-CSF by TGFbeta iPSC-dNK

582 **Figure 6. iPSC-dNK have cytotoxic activity**. **A)** Schematic of all NK effector cells (E) tested for
583 cytotoxicity against JEG3 choriocarcinoma target cells (T). **B)** Heatmap representation of mean
584 expression of Annexin+ target cells at the indicated effector-to-target (E:T) ratios. **C)** Percent
585 Annexin+ (apoptotic) $EGFR^{+}CD45^{-}$ target cells subtracted from baseline (JEG3-only) apoptosis,
586 after coculture with different effector cells at the indicated E:T ratios. Term BP, n=2 biological
587 replicates; Term CAM, n=3 biological replicates; First trimester decidua, n=3 biological replicates,
588 n = 4 technical replicates; NT iPSC-dNK n = 3 biological replicates, n=4 technical replicates; TGFβ
589 iPSC-dNK, n=3 biological replicates, n=4 technical replicates; PB-NK, n=3 biological replicates,
590 n=4 technical replicates; NK92, n=2. Three independent experiments were performed. JEG3
591 (Target cell)-only control Annexin expression included in each experiment and subtracted from all
592 samples for analysis. Statistical analysis was performed using Two-way ANOVA with Sidak's test
593 for multiple comparisons using GraphPad Prism; Data is shown as mean ± standard error. Effector
594 cell is found to be a statically significant source of variation with a ***p-value=0.0007. E:T ratio is
595 found to be a statically significant source of variation with a **p-value=0.0022. Sidak's test for
596 multiple comparisons finds Term CAM dNK vs. PBNK ** adj.p-value=0.0015; Term CAM dNK vs.
597 NK92 ** adj.p-value=0.0095; NT iPSC-dNK vs. PBNK *adj.p-value=0.05. All other pairwise
598 comparisons have p-values >0.05. Adj.p-values for all pairwise comparisons can be found in
599 **Supplementary Table 5.**

600 Alt text: Schematic illustrating all NK cell function analyzed by Killing Assay. Heat map showing
601 first trimester dNK, NT iPSC-dNK, TGFbeta iPSC-dNK, PB-NK, and NK-92 effector cells kill JEG3
602 target cells, and this increases with increasing E:T ratios. Line graphs showing the average level
603 of apoptosis above baseline cell death in target cells.

604 **Figure 7. TGFβ iPSC-dNK most closely resemble first trimester dNK.** Summary schematic of
605 key features of NK cells as measured in PB-NK and dNK across gestation and different placental
606 locations as well as the results of benchmarking NT and TGFβ iPSC-dNK against these
607 definitions.

608 Alt text: Schematic illustrating all assays used to define dNK identity and the results of assessing
609 NT and TGFbeta iPSC-dNK against these criteria.

610

611 **References**

612 1. Hyde KJ, Schust DJ. Immunologic challenges of human reproduction: an evolving story.
613 Fertil Steril. 2016 Sep 1;106(3):499-510. doi: 10.1016/j.fertnstert.2016.07.1073. Epub
614 2016 Jul 29. PMID: 27477190.
615 2. Mori M, Bogdan A, Balassa T, Csabai T, Szekeres-Bartho J. The decidua-the maternal
616 bed embracing the embryo-maintains the pregnancy. Semin Immunopathol. 2016
617 Nov;38(6):635-649. doi: 10.1007/s00281-016-0574-0. Epub 2016 Jun 10. PMID:
618 27287066; PMCID: PMC5065593.
619 3. Liu S, Diao L, Huang C, Li Y, Zeng Y, Kwak-Kim JYH. The role of decidual immune cells
620 on human pregnancy. J Reprod Immunol. 2017 Nov;124:44-53. doi:
621 10.1016/j.jri.2017.10.045. Epub 2017 Oct 18. PMID: 29055791.
622 4. Muter J, Kong CS, Brosens JJ. The Role of Decidual Subpopulations in Implantation,
623 Menstruation and Miscarriage. Front Reprod Health. 2021 Dec 23;3:804921. doi:
624 10.3389/frph.2021.804921. PMID: 36303960; PMCID: PMC9580781.
625 5. James JL, Carter AM, Chamley LW. Human placentation from nidation to 5 weeks of
626 gestation. Part I: What do we know about formative placental development following
627 implantation? Placenta. 2012 May;33(5):327-34. doi: 10.1016/j.placenta.2012.01.020.
628 Epub 2012 Feb 26. PMID: 22374510.
629 6. Yeh CC, Chao KC, Huang SJ. Innate immunity, decidual cells, and preeclampsia.
630 Reprod Sci. 2013 Apr;20(4):339-53. doi: 10.1177/1933719112450330. Epub 2012 Jul
631 18. PMID: 22814099; PMCID: PMC3823393.
632 7. Lash GE, Bulmer JN. Do uterine natural killer (uNK) cells contribute to female
633 reproductive disorders? J Reprod Immunol. 2011 Mar;88(2):156-64. doi:
634 10.1016/j.jri.2011.01.003. Epub 2011 Feb 21. PMID: 21334072.
635 8. Murphy SP, Fast LD, Hanna NN, Sharma S. Uterine NK cells mediate inflammation-
636 induced fetal demise in IL-10-null mice. J Immunol. 2005 Sep 15;175(6):4084-90. doi:
637 10.4049/jimmunol.175.6.4084. PMID: 16148158.
638 9. Murphy SP, Hanna NN, Fast LD, Shaw SK, Berg G, Padbury JF, Romero R, Sharma S.
639 Evidence for participation of uterine natural killer cells in the mechanisms responsible for
640 spontaneous preterm labor and delivery. Am J Obstet Gynecol. 2009 Mar;200(3):308.e1-

641 9. doi: 10.1016/j.ajog.2008.10.043. Epub 2008 Dec 27. PMID: 19114277; PMCID:
642 PMC3893044.
643 10. Koopman LA, Kopcow HD, Rybalov B, Boyson JE, Orange JS, Schatz F, Masch R,
644 Lockwood CJ, Schachter AD, Park PJ, Strominger JL. Human decidual natural killer
645 cells are a unique NK cell subset with immunomodulatory potential. J Exp Med. 2003
646 Oct 20;198(8):1201-12. doi: 10.1084/jem.20030305. PMID: 14568979; PMCID:
647 PMC2194228.
648 11. Strunz B, Bister J, Jönsson H, Filipovic I, Crona-Guterstam Y, Kvedaraite E, Sleiers N,
649 Dumitrescu B, Brännström M, Lentini A, Reinius B, Cornillet M, Willinger T, Gidlöf S,
650 Hamilton RS, Ivarsson MA, Björkström NK. Continuous human uterine NK cell
651 differentiation in response to endometrial regeneration and pregnancy. Sci Immunol.
652 2021 Feb 19;6(56):eabb7800. doi: 10.1126/sciimmunol.abb7800. Epub 2021 Feb 19.
653 PMID: 33617461.
654 12. Gonzalez VD, Huang YW, Delgado-Gonzalez A, Chen SY, Donoso K, Sachs K, Gentles
655 AJ, Allard GM, Kolahi KS, Howitt BE, Porpiglia E, Fantl WJ. High-grade serous ovarian
656 tumor cells modulate NK cell function to create an immune-tolerant microenvironment.
657 Cell Rep. 2021 Aug 31;36(9):109632. doi: 10.1016/j.celrep.2021.109632. PMID:
658 34469729; PMCID: PMC8546503.
659 13. de Mendonça Vieira R, Meagher A, Crespo ÂC, Kshirsagar SK, Iyer V, Norwitz ER,
660 Strominger JL, Tilburgs T. Human Term Pregnancy Decidual NK Cells Generate Distinct
661 Cytotoxic Responses. J Immunol. 2020 Jun 15;204(12):3149-3159. doi:
662 10.4049/jimmunol.1901435. Epub 2020 May 6. PMID: 32376646; PMCID: PMC7322730.
663 14. Kulkarni S, Martin MP, Carrington M. The Yin and Yang of HLA and KIR in human
664 disease. Semin Immunol. 2008 Dec;20(6):343-52. doi: 10.1016/j.smim.2008.06.003.
665 Epub 2008 Jul 16. PMID: 18635379; PMCID: PMC3501819.
666 15. Tilburgs T, Crespo ÂC, van der Zwan A, Rybalov B, Raj T, Stranger B, Gardner L,
667 Moffett A, Strominger JL. Human HLA-G+ extravillous trophoblasts: Immune-activating
668 cells that interact with decidual leukocytes. Proc Natl Acad Sci U S A. 2015 Jun
669 9;112(23):7219-24. doi: 10.1073/pnas.1507977112. Epub 2015 May 26. PMID:
670 26015573; PMCID: PMC4466754.
671 16. Hanna J, Goldman-Wohl D, Hamani Y, Avraham I, Greenfield C, Natanson-Yaron S,
672 Prus D, Cohen-Daniel L, Arnon TI, Manaster I, Gazit R, Yutkin V, Benharroch D,
673 Porgador A, Keshet E, Yagel S, Mandelboim O. Decidual NK cells regulate key
674 developmental processes at the human fetal-maternal interface. Nat Med. 2006
675 Sep;12(9):1065-74. doi: 10.1038/nm1452. Epub 2006 Aug 6. PMID: 16892062.
676 17. Kopcow HD, Allan DS, Chen X, Rybalov B, Andzelm MM, Ge B, Strominger JL. Human
677 decidual NK cells form immature activating synapses and are not cytotoxic. Proc Natl
678 Acad Sci U S A. 2005 Oct 25;102(43):15563-8. doi: 10.1073/pnas.0507835102. Epub
679 2005 Oct 17. PMID: 16230631; PMCID: PMC1266146.
680 18. Co EC, Gormley M, Kapidzic M, Rosen DB, Scott MA, Stolp HA, McMaster M, Lanier LL,
681 Bárcena A, Fisher SJ. Maternal decidual macrophages inhibit NK cell killing of invasive
682 cytotrophoblasts during human pregnancy. Biol Reprod. 2013 Jun 20;88(6):155. doi:
683 10.1095/biolreprod.112.099465. PMID: 23553431; PMCID: PMC4070869.

19. Vitale M, Bottino C, Sivori S, Sanseverino L, Castriconi R, Marcenaro E, Augugliaro R, Moretta L, Moretta A. NKp44, a novel triggering surface molecule specifically expressed by activated natural killer cells, is involved in non-major histocompatibility complex-restricted tumor cell lysis. J Exp Med. 1998 Jun 15;187(12):2065-72. doi: 10.1084/jem.187.12.2065. PMID: 9625766; PMCID: PMC2212362.
20. Borrego F, Robertson MJ, Ritz J, Peña J, Solana R. CD69 is a stimulatory receptor for natural killer cell and its cytotoxic effect is blocked by CD94 inhibitory receptor. Immunology. 1999 May;97(1):159-65. doi: 10.1046/j.1365-2567.1999.00738.x. PMID: 10447727; PMCID: PMC2326810.
21. Welte S, Kuttruff S, Waldhauer I, Steinle A. Mutual activation of natural killer cells and monocytes mediated by NKp80-AICL interaction. Nat Immunol. 2006 Dec;7(12):1334-42. doi: 10.1038/ni1402. Epub 2006 Oct 22. PMID: 17057721.
22. Vento-Tormo R, Efremova M, Botting RA, Turco MY, Vento-Tormo M, Meyer KB, Park JE, Stephenson E, Polański K, Goncalves A, Gardner L, Holmqvist S, Henriksson J, Zou A, Sharkey AM, Millar B, Innes B, Wood L, Wilbrey-Clark A, Payne RP, Ivarsson MA, Lisgo S, Filby A, Rowitch DH, Bulmer JN, Wright GJ, Stubbington MJT, Haniffa M, Moffett A, Teichmann SA. Single-cell reconstruction of the early maternal-fetal interface in humans. Nature. 2018 Nov;563(7731):347-353. doi: 10.1038/s41586-018-0698-6. Epub 2018 Nov 14. PMID: 30429548; PMCID: PMC7612850.
23. Huhn O, Ivarsson MA, Gardner L, Hollinshead M, Stinchcombe JC, Chen P, Shreeve N, Chazara O, Farrell LE, Theorell J, Ghadially H, Parham P, Griffiths G, Horowitz A, Moffett A, Sharkey AM, Colucci F. Distinctive phenotypes and functions of innate lymphoid cells in human decidua during early pregnancy. Nat Commun. 2020 Jan 20;11(1):381. doi: 10.1038/s41467-019-14123-z. PMID: 31959757; PMCID: PMC6971012.
24. Whettlock EM, Woon EV, Cuff AO, Browne B, Johnson MR, Male V. Dynamic Changes in Uterine NK Cell Subset Frequency and Function Over the Menstrual Cycle and Pregnancy. Front Immunol. 2022 Jun 16;13:880438. doi: 10.3389/fimmu.2022.880438. PMID: 35784314; PMCID: PMC9245422.
25. Zhang H, Vijayan D, Li XY, Robson SC, Geetha N, Teng MWL, Smyth MJ. The role of NK cells and CD39 in the immunological control of tumor metastases. Oncoimmunology. 2019 Apr 2;8(6):e1593809. doi: 10.1080/2162402X.2019.1593809. PMID: 31069159; PMCID: PMC6492967.
26. Sadhu C, Harris EA, Staunton DE. Enhancement of Natural Killer cell cytotoxicity by a CD18 integrin-activating antibody. Biochem Biophys Res Commun. 2007 Jul 6;358(3):938-41. doi: 10.1016/j.bbrc.2007.05.031. Epub 2007 May 14. PMID: 17512497.
27. Montaldo E, Vacca P, Chiossone L, Croxatto D, Loiacono F, Martini S, Ferrero S, Walzer T, Moretta L, Mingari MC. Unique Eomes(+) NK Cell Subsets Are Present in Uterus and Decidua During Early Pregnancy. Front Immunol. 2016 Jan 7;6:646. doi: 10.3389/fimmu.2015.00646. PMID: 27004067; PMCID: PMC4794975.
28. Marquardt N, Kekäläinen E, Chen P, Lourda M, Wilson JN, Scharenberg M, Bergman P, Al-Ameri M, Hård J, Mold JE, Ljunggren HG, Michaëlsson J. Unique transcriptional and protein-expression signature in human lung tissue-resident NK cells. Nat Commun. 2019

727 Aug 26;10(1):3841. doi: 10.1038/s41467-019-11632-9. PMID: 39378091; PMCID:
728 PMC6710242.
729 29. Soncin F, Natale D, Parast MM. Signaling pathways in mouse and human trophoblast
730 differentiation: a comparative review. Cell Mol Life Sci. 2015 Apr;72(7):1291-302. doi:
731 10.1007/s00018-014-1794-x. Epub 2014 Nov 28. PMID: 25430479; PMCID:
732 PMC4366325.
733 30. Madeja Z, Yadi H, Apps R, Boulenouar S, Roper SJ, Gardner L, Moffett A, Colucci F,
734 Hemberger M. Paternal MHC expression on mouse trophoblast affects uterine
735 vascularization and fetal growth. Proc Natl Acad Sci U S A. 2011 Mar 8;108(10):4012-7.
736 doi: 10.1073/pnas.1005342108. Epub 2011 Feb 7. PMID: 21300875; PMCID:
737 PMC3053985.
738 31. Faas MM, de Vos P. Uterine NK cells and macrophages in pregnancy. Placenta. 2017
739 Aug;56:44-52. doi: 10.1016/j.placenta.2017.03.001. Epub 2017 Mar 2. PMID: 28284455.
740 32. Fu B, Wei H. Decidual natural killer cells and the immune microenvironment at the
741 maternal-fetal interface. Sci China Life Sci. 2016 Dec;59(12):1224-1231. doi:
742 10.1007/s11427-016-0337-1. Epub 2016 Nov 29. PMID: 27905000.
743 33. Crespo ÂC, van der Zwan A, Ramalho-Santos J, Strominger JL, Tilburgs T. Cytotoxic
744 potential of decidual NK cells and CD8+ T cells awakened by infections. J Reprod
745 Immunol. 2017 Feb;119:85-90. doi: 10.1016/j.jri.2016.08.001. Epub 2016 Aug 2. PMID:
746 27523927; PMCID: PMC5290261.
747 34. Cerdeira AS, Rajakumar A, Royle CM, Lo A, Husain Z, Thadhani RI, Sukhatme VP,
748 Karumanchi SA, Kopcow HD. Conversion of peripheral blood NK cells to a decidual NK-
749 like phenotype by a cocktail of defined factors. J Immunol. 2013 Apr 15;190(8):3939-48.
750 doi: 10.4049/jimmunol.1202582. Epub 2013 Mar 13. PMID: 23487420; PMCID:
751 PMC3742368.
752 35. Cavalli RC, Cerdeira AS, Pernicone E, Korkes HA, Burke SD, Rajakumar A, Thadhani
753 RI, Roberts DJ, Bhasin M, Karumanchi SA, Kopcow HD. Induced Human Decidual NK-
754 Like Cells Improve Utero-Placental Perfusion in Mice. PLoS One. 2016 Oct
755 13;11(10):e0164353. doi: 10.1371/journal.pone.0164353. PMID: 27736914; PMCID:
756 PMC5063315.
757 36. Cerneckis J, Cai H, Shi Y. Induced pluripotent stem cells (iPSCs): molecular
758 mechanisms of induction and applications. Signal Transduct Target Ther. 2024 Apr
759 26;9(1):112. doi: 10.1038/s41392-024-01809-0. PMID: 38670977; PMCID:
760 PMC11053163.
761 37. Morey R, Bui T, Cheung VC, Dong C, Zemke JE, Requena D, Arora H, Jackson MG,
762 Pizzo D, Theunissen TW, Horii M. iPSC-based modeling of preeclampsia identifies
763 epigenetic defects in extravillous trophoblast differentiation. iScience. 2024 Mar
764 25;27(4):109569. doi: 10.1016/j.isci.2024.109569. PMID: 38623329; PMCID:
765 PMC11016801.
766 38. Cheung VC, Bui T, Soncin F, Bai T, Kessler JA, Parast MM, Horii M. Current Strategies
767 of Modeling Human Trophoblast Using Human Pluripotent Stem Cells in vitro. Curr
768 Protoc. 2023 Oct;3(10):e875. doi: 10.1002/cpz1.875. Erratum in: Curr Protoc. 2024
769 Apr;4(4):e1049. doi: 10.1002/cpz1.1049. PMID: 37787612; PMCID: PMC10558083.

39. Morey R, Bui T, Fisch KM, Horii M. Modeling placental development and disease using human pluripotent stem cells. Placenta. 2023 Sep 26;141:18-25. doi: 10.1016/j.placenta.2022.10.011. Epub 2022 Oct 31. PMID: 36333266; PMCID: PMC10148925.
40. Wu Y, Sun T, Medina P, Narasimhan P, Stevenson DK, Von Versen-Höynck F, Armstrong J, Wu JC, Sayed N, Winn VD. A Novel Stem Cell Model to Study Preeclampsia Endothelial Dysfunction. Reprod Sci. 2024 Oct;31(10):2993-3003. doi: 10.1007/s43032-024-01590-z. Epub 2024 Aug 23. PMID: 39179924; PMCID: PMC11438721.
41. Goldenson BH, Zhu H, Wang YM, Heragu N, Bernareggi D, Ruiz-Cisneros A, Bahena A, Ask EH, Hoel HJ, Malmberg KJ, Kaufman DS. Umbilical Cord Blood and iPSC-Derived Natural Killer Cells Demonstrate Key Differences in Cytotoxic Activity and KIR Profiles. Front Immunol. 2020 Oct 15;11:561553. doi: 10.3389/fimmu.2020.561553. PMID: 33178188; PMCID: PMC7593774.
42. Bock AM, Knorr D, Kaufman DS. Development, expansion, and in vivo monitoring of human NK cells from human embryonic stem cells (hESCs) and and induced pluripotent stem cells (iPSCs). J Vis Exp. 2013 Apr 23;(74):e50337. doi: 10.3791/50337. PMID: 23644738; PMCID: PMC3667548.
43. Thangaraj JL, Coffey M, Lopez E, Kaufman DS. Disruption of TGF-β signaling pathway is required to mediate effective killing of hepatocellular carcinoma by human iPSC-derived NK cells. Cell Stem Cell. 2024 Sep 5;31(9):1327-1343.e5. doi: 10.1016/j.stem.2024.06.009. Epub 2024 Jul 9. PMID: 38986609; PMCID: PMC11380586.
44. Goldenson BH, Hor P, Kaufman DS. iPSC-Derived Natural Killer Cell Therapies - Expansion and Targeting. Front Immunol. 2022 Feb 3;13:841107. doi: 10.3389/fimmu.2022.841107. PMID: 35185932; PMCID: PMC8851389.
45. Tao Y, Li YH, Zhang D, Xu L, Chen JJ, Sang YF, Piao HL, Jing XL, Yu M, Fu Q, Zhou ST, Li DJ, Du MR. Decidual $CXCR4^{+}$ $CD56^{bright}$ NK cells as a novel NK subset in maternal-foetal immune tolerance to alleviate early pregnancy failure. Clin Transl Med. 2021 Oct;11(10):e540. doi: 10.1002/ctm2.540. PMID: 34709764; PMCID: PMC8516340.
46. Tatematsu BK, Sojka DK. Tissue-resident natural killer cells derived from conventional natural killer cells are regulated by progesterone in the uterus. Mucosal Immunol. 2025 Apr;18(2):390-401. doi: 10.1016/j.mucimm.2024.12.009. Epub 2024 Dec 19. PMID: 39708955.
47. Jauniaux E, Watson AL, Hempstock J, Bao YP, Skepper JN, Burton GJ. Onset of maternal arterial blood flow and placental oxidative stress. A possible factor in human early pregnancy failure. Am J Pathol. 2000 Dec;157(6):2111-22. doi: 10.1016/S0002-9440(10)64849-3. PMID: 11106583; PMCID: PMC1885754.
48. Hanna J, Wald O, Goldman-Wohl D, Prus D, Markel G, Gazit R, Katz G, Haimov-Kochman R, Fujii N, Yagel S, Peled A, Mandelboim O. CXCL12 expression by invasive trophoblasts induces the specific migration of CD16- human natural killer cells. Blood. 2003 Sep 1;102(5):1569-77. doi: 10.1182/blood-2003-02-0517. Epub 2003 May 1. PMID: 12730110.

49. Pique-Regi R, Romero R, Tarca AL, Sendler ED, Xu Y, Garcia-Flores V, Leng Y, Luca F, Hassan SS, Gomez-Lopez N. Single cell transcriptional signatures of the human placenta in term and preterm parturition. Elife. 2019 Dec 12;8:e52004. doi: 10.7554/eLife.52004. PMID: 31829938; PMCID: PMC6949028.
50. Zhu H, Kaufman DS. An Improved Method to Produce Clinical-Scale Natural Killer Cells from Human Pluripotent Stem Cells. Methods Mol Biol. 2019;2048:107-119. doi: 10.1007/978-1-4939-9728-2_12. PMID: 31396935.
51. Fauriat C, Long EO, Ljunggren HG, Bryceson YT. Regulation of human NK-cell cytokine and chemokine production by target cell recognition. Blood. 2010 Mar 18;115(11):2167-76. doi: 10.1182/blood-2009-08-238469. Epub 2009 Dec 1. PMID: 19965656; PMCID: PMC2844017.
52. Wiedemann GM, Grassmann S, Lau CM, Rapp M, Villarino AV, Friedrich C, Gasteiger G, O'Shea JJ, Sun JC. Divergent Role for STAT5 in the Adaptive Responses of Natural Killer Cells. Cell Rep. 2020 Dec 15;33(11):108498. doi: 10.1016/j.celrep.2020.108498. PMID: 33326784; PMCID: PMC7773031.
53. Gotthardt D, Trifinopoulos J, Sexl V, Putz EM. JAK/STAT Cytokine Signaling at the Crossroad of NK Cell Development and Maturation. Front Immunol. 2019 Nov 12;10:2590. doi: 10.3389/fimmu.2019.02590. PMID: 31781102; PMCID: PMC6861185.
54. Zhang YE. Non-Smad pathways in TGF-beta signaling. Cell Res. 2009 Jan;19(1):128-39. doi: 10.1038/cr.2008.328. PMID: 19114990; PMCID: PMC2635127.
55. Liu X, Aneas I, Sakabe N, Anderson RL, Billstrand C, Paz C, Kaur H, Furner B, Choi S, Prichina AY, Enninga EAL, Dong H, Murtha A, Crawford GE, Kessler JA, Grobman W, Nobrega MA, Rana S, Ober C. Single cell profiling at the maternal-fetal interface reveals a deficiency of PD-L1+ non-immune cells in human spontaneous preterm labor. Sci Rep. 2023 May 16;13(1):7903. doi: 10.1038/s41598-023-35051-5. PMID: 37193763; PMCID: PMC10188528.
56. Garcia-Flores V, Romero R, Tarca AL, Peyvandipour A, Xu Y, Galaz J, Miller D, Chaiworapongsa T, Chaemsaithong P, Berry SM, Awonuga AO, Bryant DR, Pique-Regi R, Gomez-Lopez N. Deciphering maternal-fetal cross-talk in the human placenta during parturition using single-cell RNA sequencing. Sci Transl Med. 2024 Jan 10;16(729):eadh8335. doi: 10.1126/scitranslmed.adh8335. Epub 2024 Jan 10. PMID: 38198568; PMCID: PMC11238316.
57. Viel S, Marçais A, Guimaraes FS, Loftus R, Rabilloud J, Grau M, Degouve S, Djebali S, Sanlaville A, Charrier E, Bienvenu J, Marie JC, Caux C, Marvel J, Town L, Huntington ND, Bartholin L, Finlay D, Smyth MJ, Walzer T. TGF-β inhibits the activation and functions of NK cells by repressing the mTOR pathway. Sci Signal. 2016 Feb 16;9(415):ra19. doi: 10.1126/scisignal.aad1884. PMID: 26884601.
58. Hawke LG, Whitford MKM, Ormiston ML. The Production of Pro-angiogenic VEGF-A Isoforms by Hypoxic Human NK Cells Is Independent of Their TGF-β-Mediated Conversion to an ILC1-Like Phenotype. Front Immunol. 2020 Aug 25;11:1903. doi: 10.3389/fimmu.2020.01903. PMID: 32983113; PMCID: PMC7477355.
59. Iinuma T, Kurokawa T, Aoki T, Onodera A, Fukazawa T, Yamada D, Kitahara G, Okoshi M, Yamaguchi M, Okura H, Sasaki S, Sasako Y, Kira S, Sharif J, Tsuchiyama Y, Kobayashi M, Kobayashi N, Horikoshi T, Inaba Y, Hanaoka H, Okamoto Y, Hanazawa T,

857 Koseki H, Motohashi S. Allogeneic iPSC-derived iNKT cells in recurrent head and neck
858 cancer: a phase 1 trial. Nat Commun. 2025 Nov 26;16(1):11666. doi: 10.1038/s41467-
859 025-66801-w. PMID: 41298491; PMCID: PMC12749447.
860 60. Foltz JA, Moseman JE, Thakkar A, Chakravarti N, Lee DA. TGFβ Imprinting During
861 Activation Promotes Natural Killer Cell Cytokine Hypersecretion. Cancers (Basel). 2018
862 Nov 5;10(11):423. doi: 10.3390/cancers10110423. PMID: 30400618; PMCID:
863 PMC6267005.
864 61. Cheung VC, Peng CY, Marinić M, Sakabe NJ, Aneas I, Lynch VJ, Ober C, Nobrega MA,
865 Kessler JA. Pluripotent stem cell-derived endometrial stromal fibroblasts in a cyclic,
866 hormone-responsive, coculture model of human decidua. Cell Rep. 2021 May
867 18;35(7):109138. doi: 10.1016/j.celrep.2021.109138. PMID: 34010658.
868 62. Jameson G, Walsh A, Woods R, Batten I, Murphy DM, Connolly SA, Duffin E,
869 O'Gallchobhair O, Nadarajan P, O'Connell F, Gleeson LE, Keane J, Basdeo SA. Human
870 tissue-resident NK cells in the lung have a higher glycolytic capacity than non-tissue-
871 resident NK cells in the lung and blood. Proc Natl Acad Sci U S A. 2024 Oct
872 15;121(42):e2412489121. doi: 10.1073/pnas.2412489121. Epub 2024 Oct 8. PMID:
873 39378091; PMCID: PMC11494342.
874 63. Jaeger N, Antonova AU, Kreisel D, Roan F, Lantelme E, Ziegler SF, Cella M, Colonna
875 M. Diversity of group 1 innate lymphoid cells in human tissues. Nat Immunol. 2024
876 Aug;25(8):1460-1473. doi: 10.1038/s41590-024-01885-y. Epub 2024 Jul 2. PMID:
877 38956380.
878 64. Rebuffet L, Melsen JE, Escalière B, Basurto-Lozada D, Bhandoola A, Björkström NK,
879 Bryceson YT, Castriconi R, Cichocki F, Colonna M, Davis DM, Diefenbach A, Ding Y,
880 Haniffa M, Horowitz A, Lanier LL, Malmberg KJ, Miller JS, Moretta L, Narni-Mancinelli E,
881 O'Neill LAJ, Romagnani C, Ryan DG, Sivori S, Sun D, Vagne C, Vivier E. High-
882 dimensional single-cell analysis of human natural killer cell heterogeneity. Nat Immunol.
883 2024 Aug;25(8):1474-1488. doi: 10.1038/s41590-024-01883-0. Epub 2024 Jul 2. PMID:
884 38956378; PMCID: PMC11291291.
885 65. Hao Y, Stuart T, Kowalski MH, Choudhary S, Hoffman P, Hartman A, Srivastava A,
886 Molla G, Madad S, Fernandez-Granda C, Satija R. Dictionary learning for integrative,
887 multimodal and scalable single-cell analysis. Nat Biotechnol. 2024 Feb;42(2):293-304.
888 doi: 10.1038/s41587-023-01767-y. Epub 2023 May 25. PMID: 37231261; PMCID:
889 PMC10928517.
890 66. McGinnis CS, Murrow LM, Gartner ZJ. DoubletFinder: Doublet Detection in Single-Cell
891 RNA Sequencing Data Using Artificial Nearest Neighbors. Cell Syst. 2019 Apr
892 24;8(4):329-337.e4. doi: 10.1016/j.cels.2019.03.003. Epub 2019 Apr 3. PMID:
893 30954475; PMCID: PMC6853612.
894 67. Zappia L, Oshlack A. Clustering trees: a visualization for evaluating clusterings at
895 multiple resolutions. Gigascience. 2018 Jul 1;7(7):giy083. doi:
896 10.1093/gigascience/giy083. PMID: 30010766; PMCID: PMC6057528.
897 68. Hulsen, Tim. "DeepVenn--a web application for the creation of area-proportional Venn
898 diagrams using the deep learning framework Tensorflow. js." *arXiv preprint*
899 *arXiv:2210.04597*(2022).

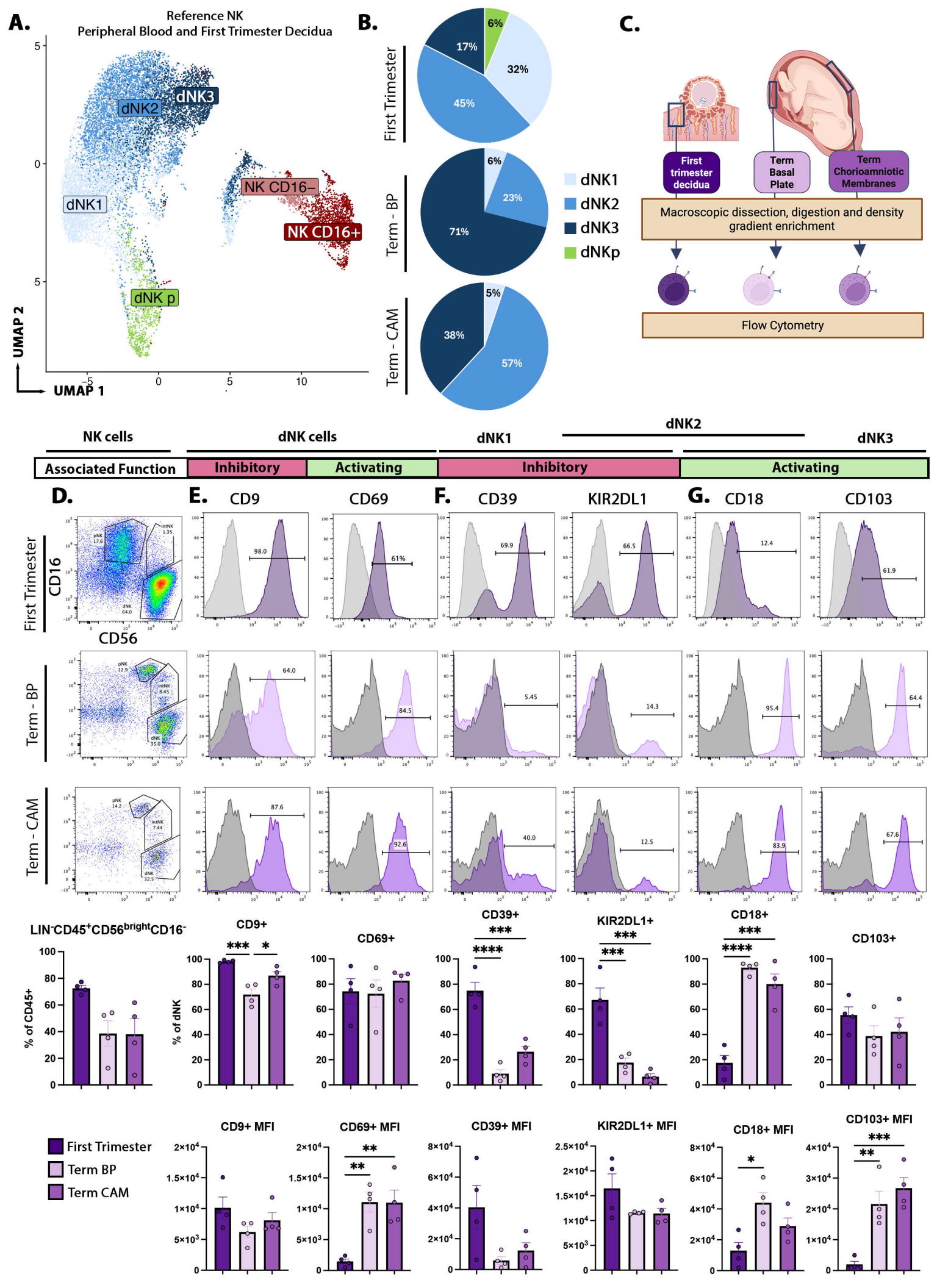
A.
Reference NK
Peripheral Blood and First Trimester Decidua
dNK1
dNK2
dNK3
dNK p
NK CD16–
NK CD16+
UMAP 1
UMAP 2
B.
First Trimester
Term - BP
Term - CAM
6%
17%
32%
45%
6%
23%
71%
5%
38%
57%
dNK1
dNK2
dNK3
dNKp
C.
First trimester decidua
Term Basal Plate
Term Chorioamniotic Membranes
Macroscopic dissection, digestion and density gradient enrichment
Flow Cytometry
NK cells
dNK cells
dNK1
dNK2
dNK3
Associated Function
Inhibitory
Activating
Inhibitory
Activating
D.
E.
CD9
CD69
F.
CD39
KIR2DL1
G.
CD18
CD103
First Trimester
Term - BP
Term - CAM
CD16
CD56
LIN-CD45+CD56bright CD16-
% of CD45+
% of dNK
CD9+
CD69+
CD39+
KIR2DL1+
CD18+
CD103+
CD9+ MFI
CD69+ MFI
CD39+ MFI
KIR2DL1+ MFI
CD18+ MFI
CD103+ MFI
First Trimester
Term BP
Term CAM

Figure 2

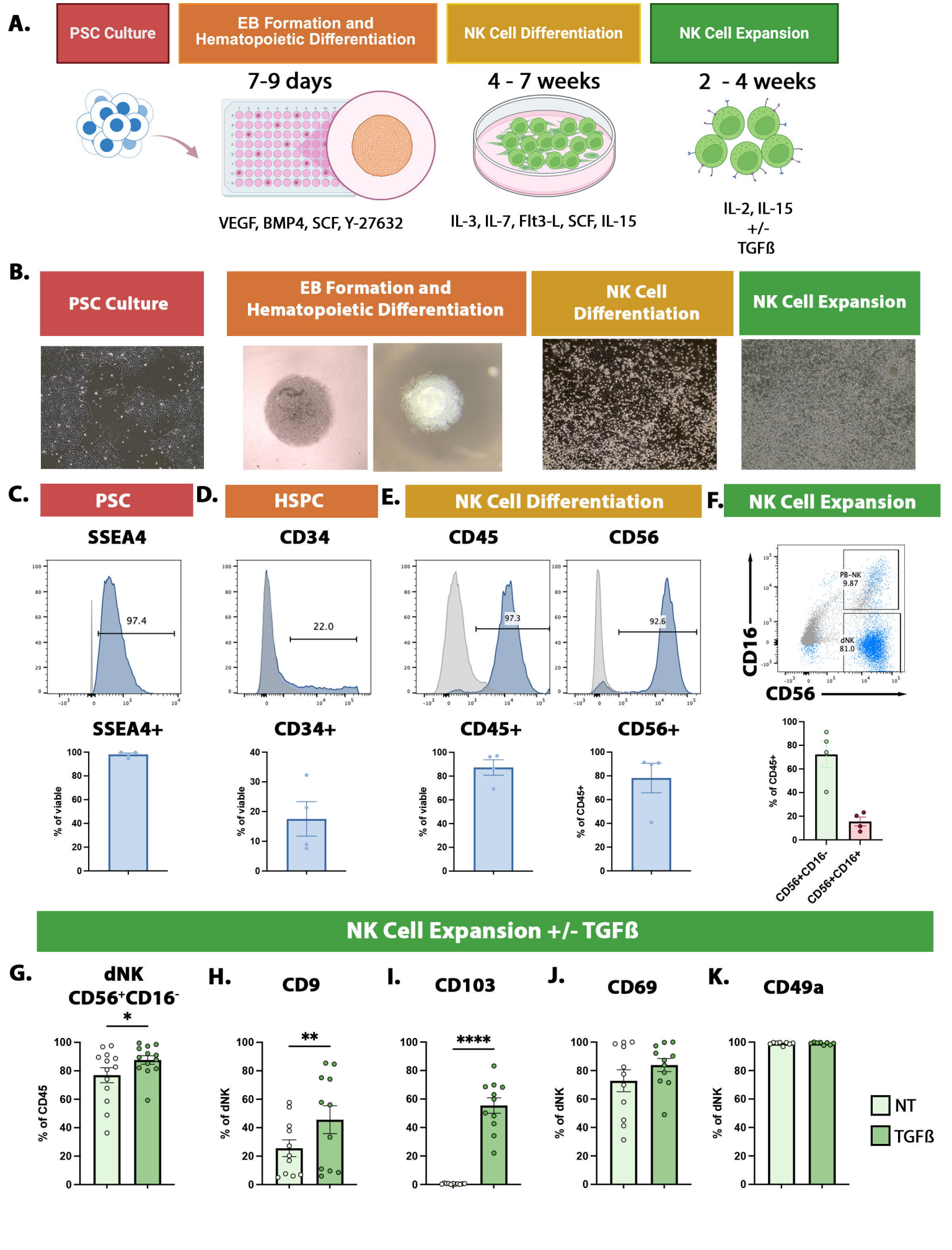
A.
PSC Culture
EB Formation and Hematopoietic Differentiation
NK Cell Differentiation
NK Cell Expansion
7-9 days
4 - 7 weeks
2 - 4 weeks
VEGF, BMP4, SCF, Y-27632
IL-3, IL-7, Flt3-L, SCF, IL-15
IL-2, IL-15 +/- TGFß
B.
PSC Culture
EB Formation and Hematopoietic Differentiation
NK Cell Differentiation
NK Cell Expansion
C.
PSC
D.
HSPC
E.
NK Cell Differentiation
F.
NK Cell Expansion
SSEA4
CD34
CD45
CD56
97.4
22.0
97.3
92.6
PB-NK 9.87
dNK 81.0
CD16
CD56
SSEA4+
CD34+
CD45+
CD56+
% of viable
% of CD45+
CD56+CD16-
CD56+CD16+
NK Cell Expansion +/- TGFß
G.
dNK CD56+CD16-
H.
CD9
I.
CD103
J.
CD69
K.
CD49a
*
**
****
% of CD45
% of dNK
NT
TGFß

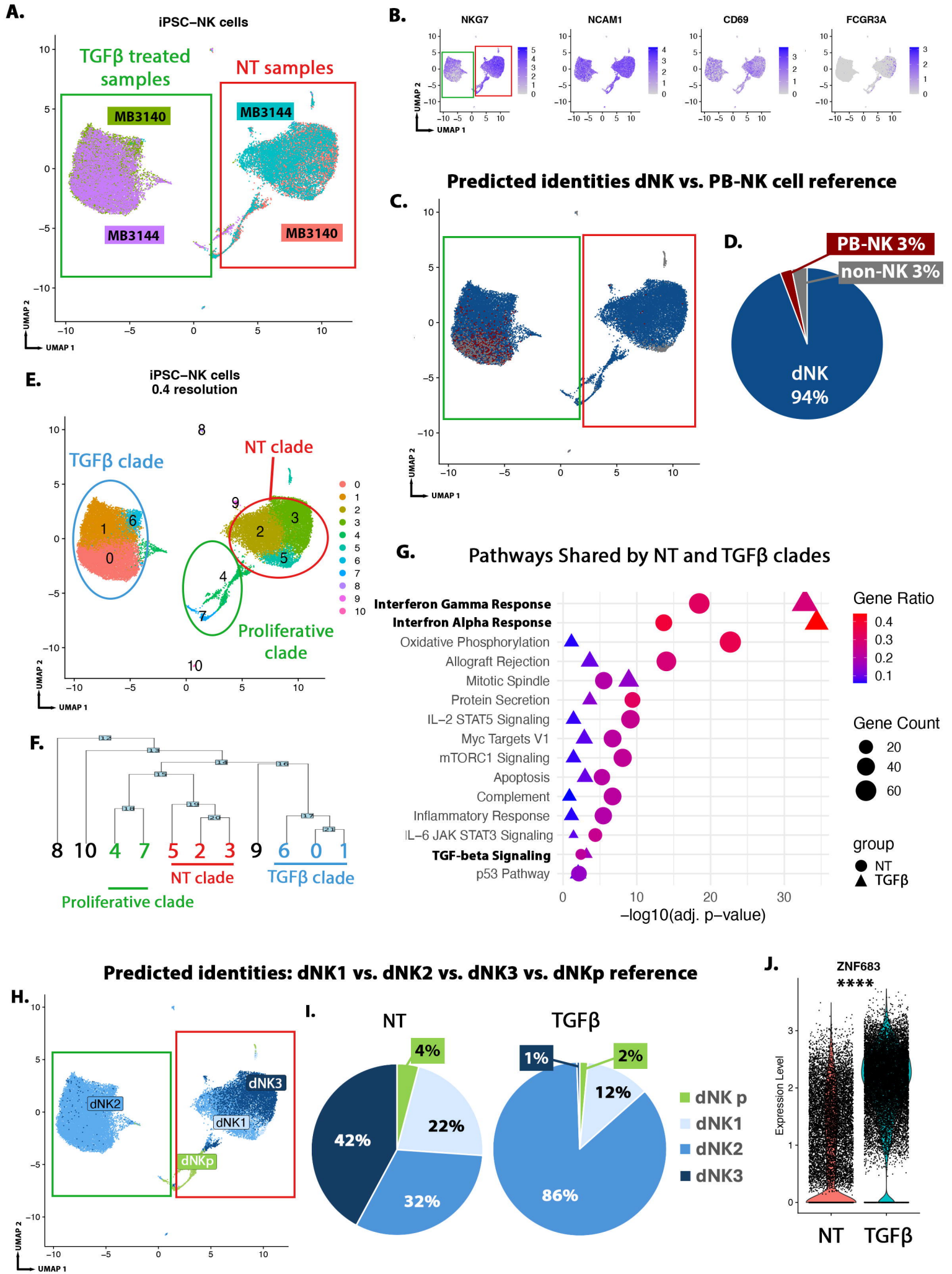
A.
iPSC–NK cells
TGFβ treated samples
NT samples
MB3140
MB3144
MB3144
MB3140
UMAP 1
UMAP 2
B.
NKG7
NCAM1
CD69
FCGR3A
UMAP 1
UMAP 2
Predicted identities dNK vs. PB-NK cell reference
C.
UMAP 1
UMAP 2
D.
PB-NK 3%
non-NK 3%
dNK 94%
E.
iPSC–NK cells 0.4 resolution
TGFβ clade
NT clade
Proliferative clade
UMAP 1
UMAP 2
F.
8 10 4 7 5 2 3 9 6 0 1
NT clade
TGFβ clade
Proliferative clade
G.
Pathways Shared by NT and TGFβ clades
Interferon Gamma Response
Interfron Alpha Response
Oxidative Phosphorylation
Allograft Rejection
Mitotic Spindle
Protein Secretion
IL–2 STAT5 Signaling
Myc Targets V1
mTORC1 Signaling
Apoptosis
Complement
Inflammatory Response
IL–6 JAK STAT3 Signaling
TGF-beta Signaling
p53 Pathway
–log10(adj. p–value)
Gene Ratio
Gene Count
group
NT
TGFβ
Predicted identities: dNK1 vs. dNK2 vs. dNK3 vs. dNKp reference
H.
dNK2
dNK3
dNK1
dNKp
UMAP 1
UMAP 2
I.
NT
TGFβ
4%
22%
32%
42%
1%
2%
12%
86%
dNK p
dNK1
dNK2
dNK3
J.
ZNF683
****
Expression Level
NT
TGFβ

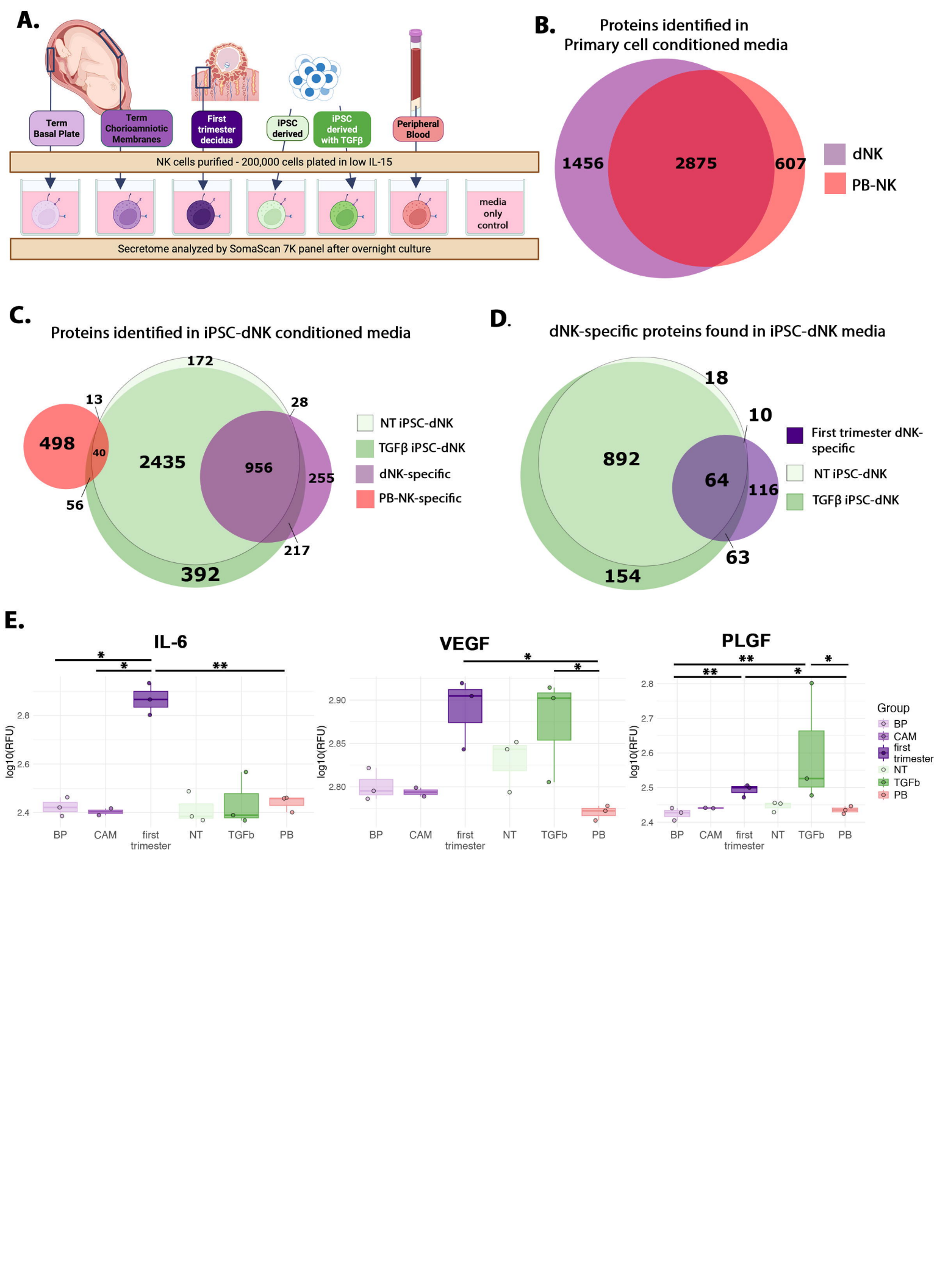
A.
Term Basal Plate
Term Chorioamniotic Membranes
First trimester decidua
iPSC derived
iPSC derived with TGFβ
Peripheral Blood
NK cells purified - 200,000 cells plated in low IL-15
media only control
Secretome analyzed by SomaScan 7K panel after overnight culture
B.
Proteins identified in Primary cell conditioned media
1456
2875
607
dNK
PB-NK
C.
Proteins identified in iPSC-dNK conditioned media
172
13
28
498
40
2435
956
255
56
217
392
NT iPSC-dNK
TGFβ iPSC-dNK
dNK-specific
PB-NK-specific
D.
dNK-specific proteins found in iPSC-dNK media
18
10
892
64
116
63
154
First trimester dNK-specific
NT iPSC-dNK
TGFβ iPSC-dNK
E.
IL-6
VEGF
PLGF
log10(RFU)
BP
CAM
first trimester
NT
TGFb
PB
Group
BP
CAM
first trimester
NT
TGFb
PB

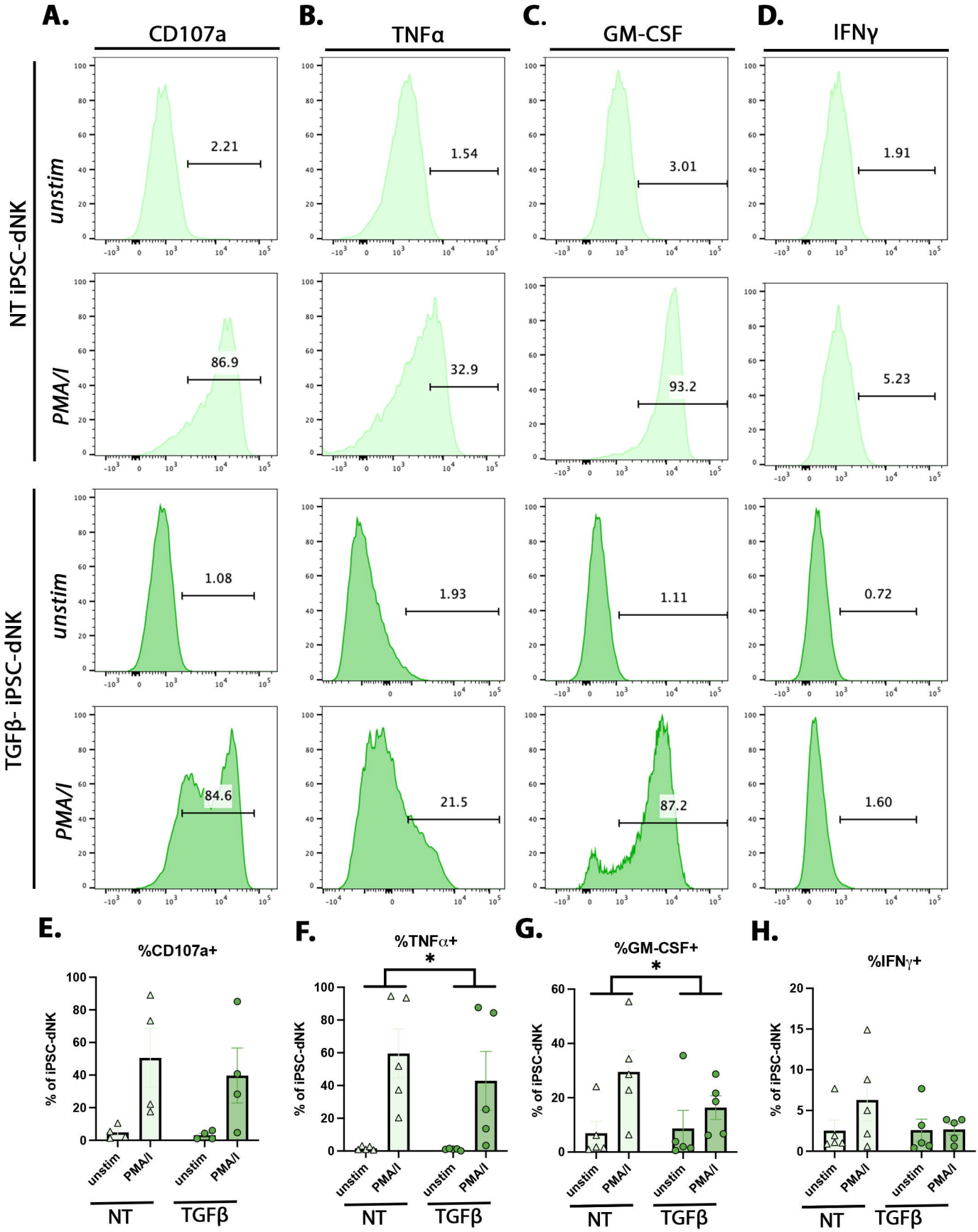
A.
CD107a
B.
TNFα
C.
GM-CSF
D.
IFNγ
NT iPSC-dNK
TGFβ- iPSC-dNK
unstim
PMA/I
2.21
1.54
3.01
1.91
86.9
32.9
93.2
5.23
1.08
1.93
1.11
0.72
84.6
21.5
87.2
1.60
E.
%CD107a+
F.
%TNFα+
G.
%GM-CSF+
H.
%IFNγ+
% of iPSC-dNK
unstim
PMA/I
NT
TGFβ
*

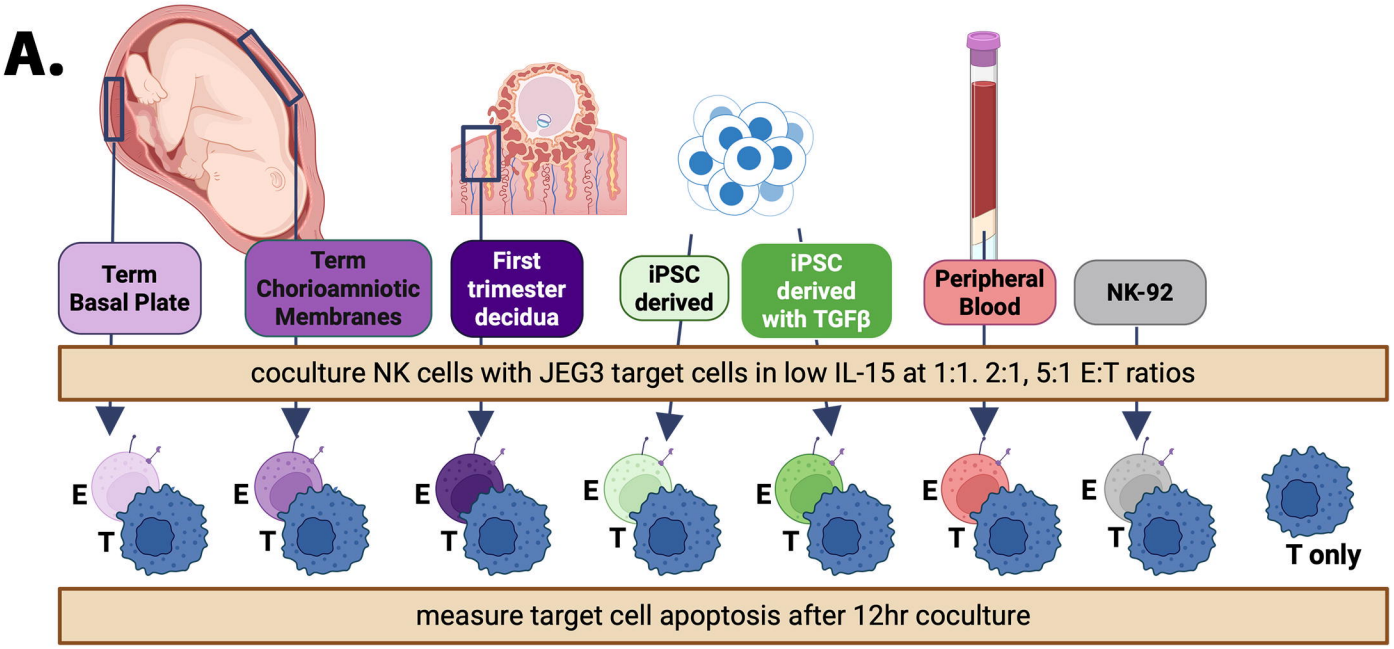
A.
Term Basal Plate
Term Chorioamniotic Membranes
First trimester decidua
iPSC derived
iPSC derived with TGFβ
Peripheral Blood
NK-92
coculture NK cells with JEG3 target cells in low IL-15 at 1:1. 2:1, 5:1 E:T ratios
E
T
T only
measure target cell apoptosis after 12hr coculture

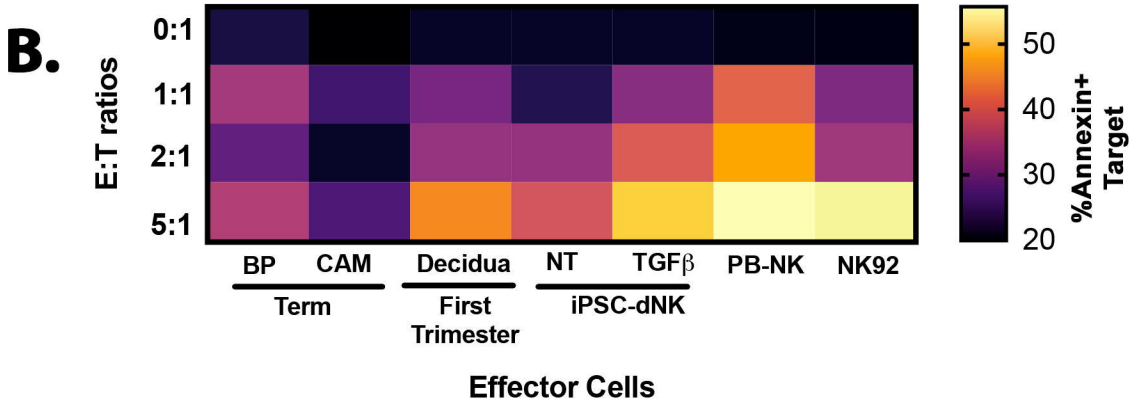
B.
E:T ratios
0:1
1:1
2:1
5:1
BP
CAM
Decidua
NT
TGFβ
PB-NK
NK92
Term
First Trimester
iPSC-dNK
Effector Cells
50
40
30
20
%Annexin+ Target

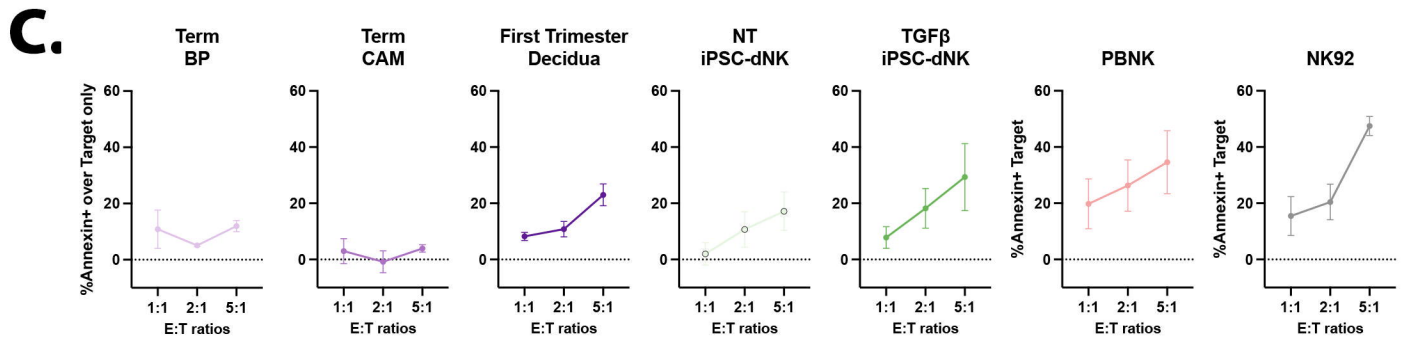
C.
Term BP
Term CAM
First Trimester Decidua
NT iPSC-dNK
TGFβ iPSC-dNK
PBNK
NK92
%Annexin+ over Target only
%Annexin+ Target
60
40
20
0
1:1
2:1
5:1
E:T ratios

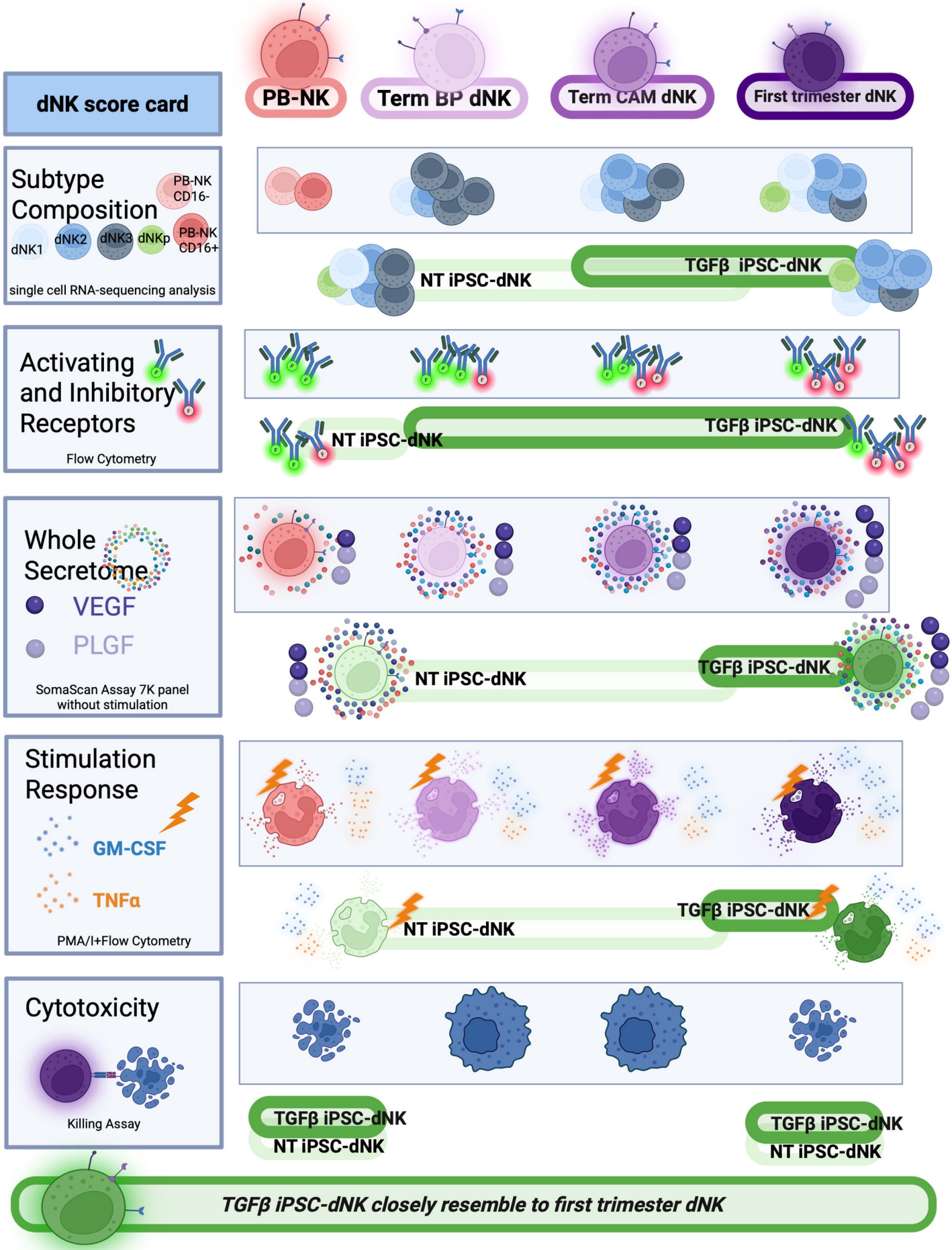
dNK score card
PB-NK
Term BP dNK
Term CAM dNK
First trimester dNK
Subtype Composition
PB-NK CD16-
dNK1
dNK2
dNK3
dNKp
PB-NK CD16+
single cell RNA-sequencing analysis
NT iPSC-dNK
TGFβ iPSC-dNK
Activating and Inhibitory Receptors
Flow Cytometry
NT iPSC-dNK
TGFβ iPSC-dNK
Whole Secretome
VEGF
PLGF
SomaScan Assay 7K panel without stimulation
NT iPSC-dNK
TGFβ iPSC-dNK
Stimulation Response
GM-CSF
TNFα
PMA/I+Flow Cytometry
NT iPSC-dNK
TGFβ iPSC-dNK
Cytotoxicity
Killing Assay
TGFβ iPSC-dNK
NT iPSC-dNK
TGFβ iPSC-dNK
NT iPSC-dNK
TGFβ iPSC-dNK closely resemble to first trimester dNK

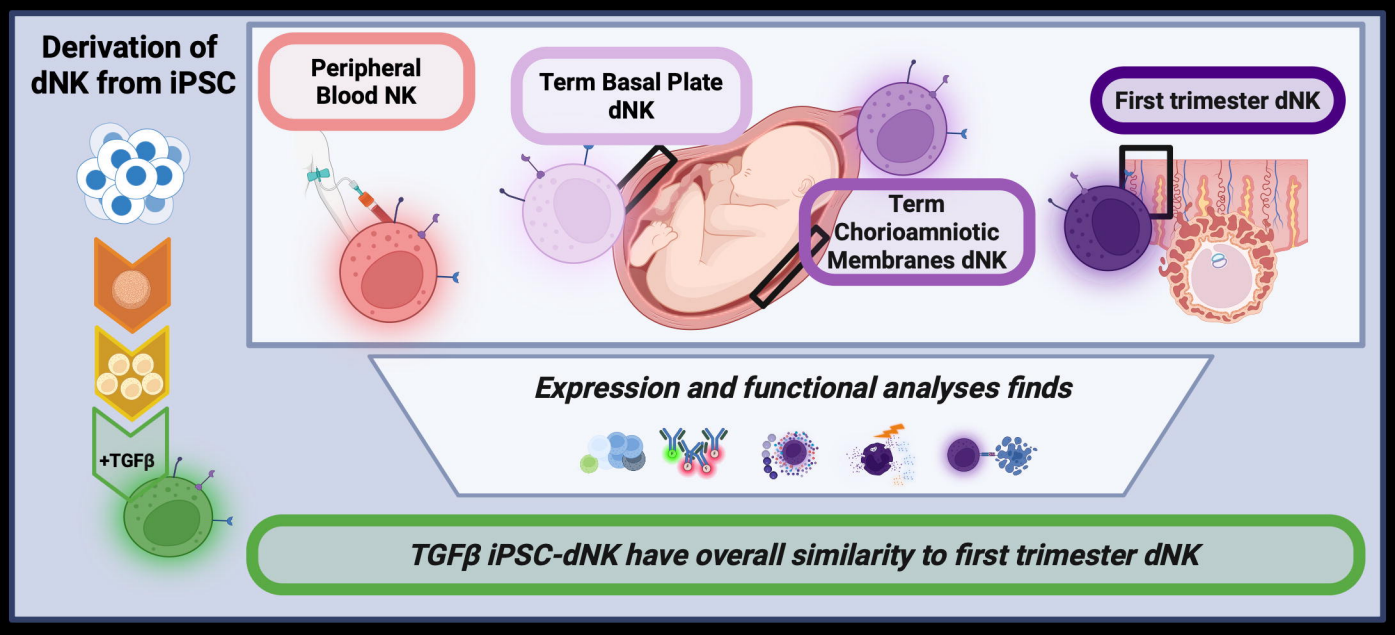
Derivation of dNK from iPSC
+TGFβ
Peripheral Blood NK
Term Basal Plate dNK
Term Chorioamniotic Membranes dNK
First trimester dNK
Expression and functional analyses finds
TGFβ iPSC-dNK have overall similarity to first trimester dNK

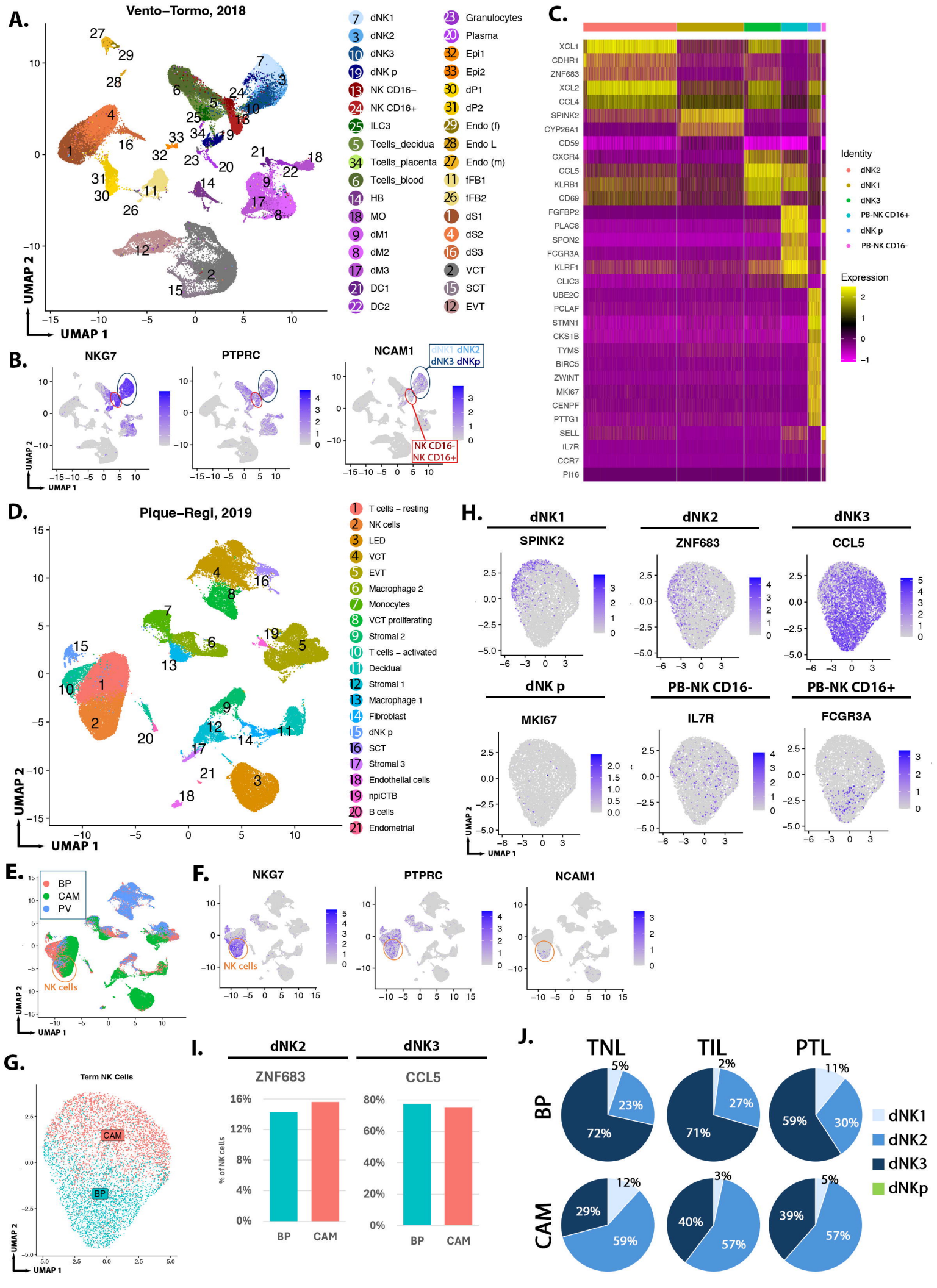
A.
Vento–Tormo, 2018
UMAP 1
UMAP 2
7 dNK1
3 dNK2
10 dNK3
19 dNK p
13 NK CD16–
24 NK CD16+
25 ILC3
5 Tcells_decidua
34 Tcells_placenta
6 Tcells_blood
14 HB
18 MO
9 dM1
8 dM2
17 dM3
21 DC1
22 DC2
23 Granulocytes
20 Plasma
32 Epi1
33 Epi2
30 dP1
31 dP2
29 Endo (f)
28 Endo L
27 Endo (m)
11 fFB1
26 fFB2
1 dS1
4 dS2
16 dS3
2 VCT
15 SCT
12 EVT
B.
NKG7
PTPRC
NCAM1
dNK1 dNK2
dNK3 dNKp
NK CD16-
NK CD16+
C.
XCL1
CDHR1
ZNF683
XCL2
CCL4
SPINK2
CYP26A1
CD59
CXCR4
CCL5
KLRB1
CD69
FGFBP2
PLAC8
SPON2
FCGR3A
KLRF1
CLIC3
UBE2C
PCLAF
STMN1
CKS1B
TYMS
BIRC5
ZWINT
MKI67
CENPF
PTTG1
SELL
IL7R
CCR7
PI16
Identity
dNK2
dNK1
dNK3
PB-NK CD16+
dNK p
PB-NK CD16-
Expression
D.
Pique–Regi, 2019
1 T cells – resting
2 NK cells
3 LED
4 VCT
5 EVT
6 Macrophage 2
7 Monocytes
8 VCT proliferating
9 Stromal 2
10 T cells – activated
11 Decidual
12 Stromal 1
13 Macrophage 1
14 Fibroblast
15 dNK p
16 SCT
17 Stromal 3
18 Endothelial cells
19 npiCTB
20 B cells
21 Endometrial
H.
dNK1
SPINK2
dNK2
ZNF683
dNK3
CCL5
dNK p
MKI67
PB-NK CD16-
IL7R
PB-NK CD16+
FCGR3A
E.
BP
CAM
PV
NK cells
F.
NKG7
PTPRC
NCAM1
NK cells
G.
Term NK Cells
CAM
BP
I.
dNK2
ZNF683
dNK3
CCL5
% of NK cells
BP
CAM
J.
TNL
TIL
PTL
BP
CAM
5%
23%
72%
2%
27%
71%
11%
30%
59%
12%
29%
59%
3%
40%
57%
5%
39%
57%
dNK1
dNK2
dNK3
dNKp

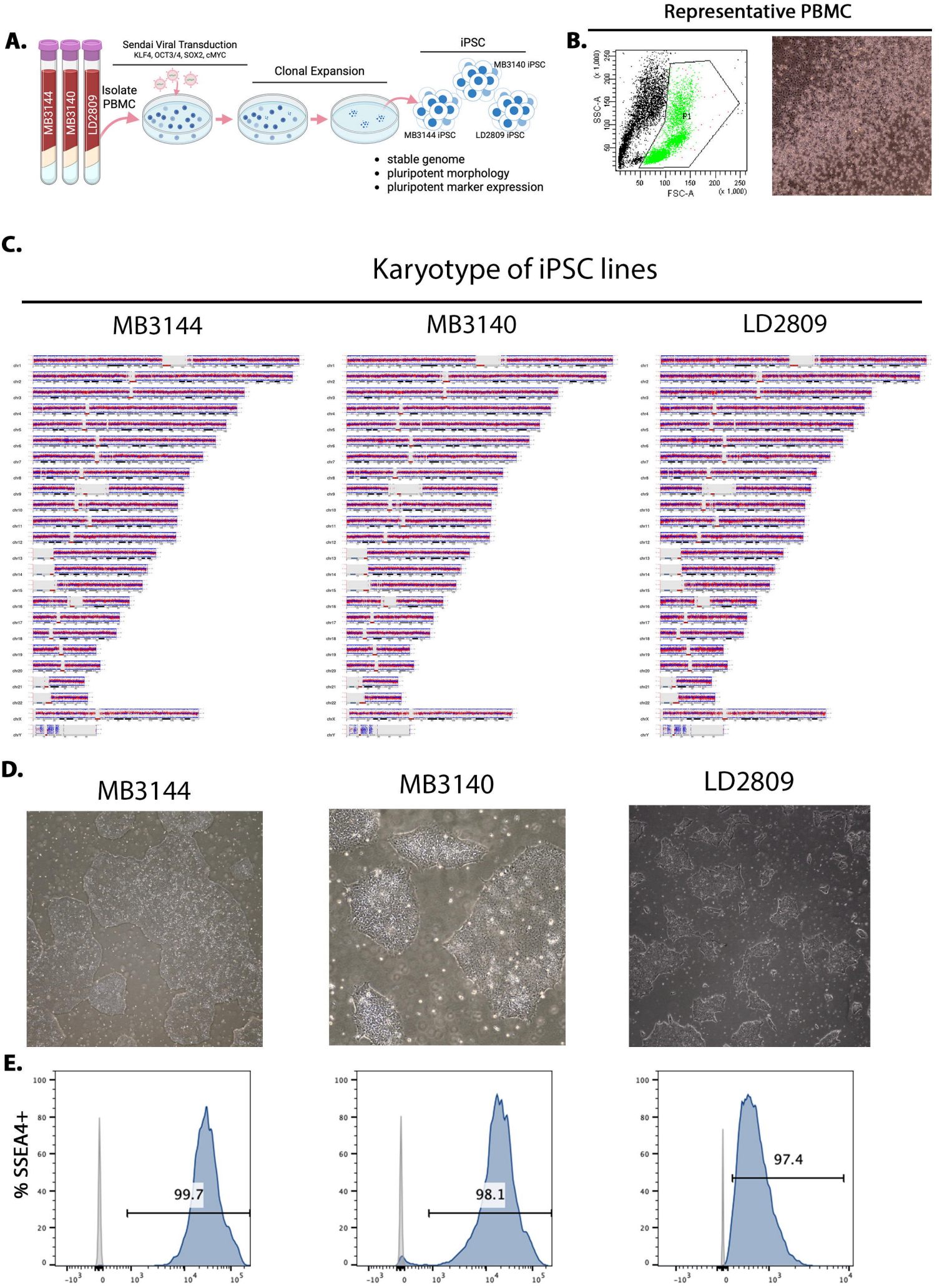
A.
MB3144
MB3140
LD2809
Isolate PBMC
Sendai Viral Transduction
KLF4, OCT3/4, SOX2, cMYC
Clonal Expansion
iPSC
MB3140 iPSC
MB3144 iPSC
LD2809 iPSC
stable genome
pluripotent morphology
pluripotent marker expression
B.
Representative PBMC
SSC-A
FSC-A
P1
C.
Karyotype of iPSC lines
MB3144
MB3140
LD2809
D.
MB3144
MB3140
LD2809
E.
% SSEA4+
99.7
98.1
97.4

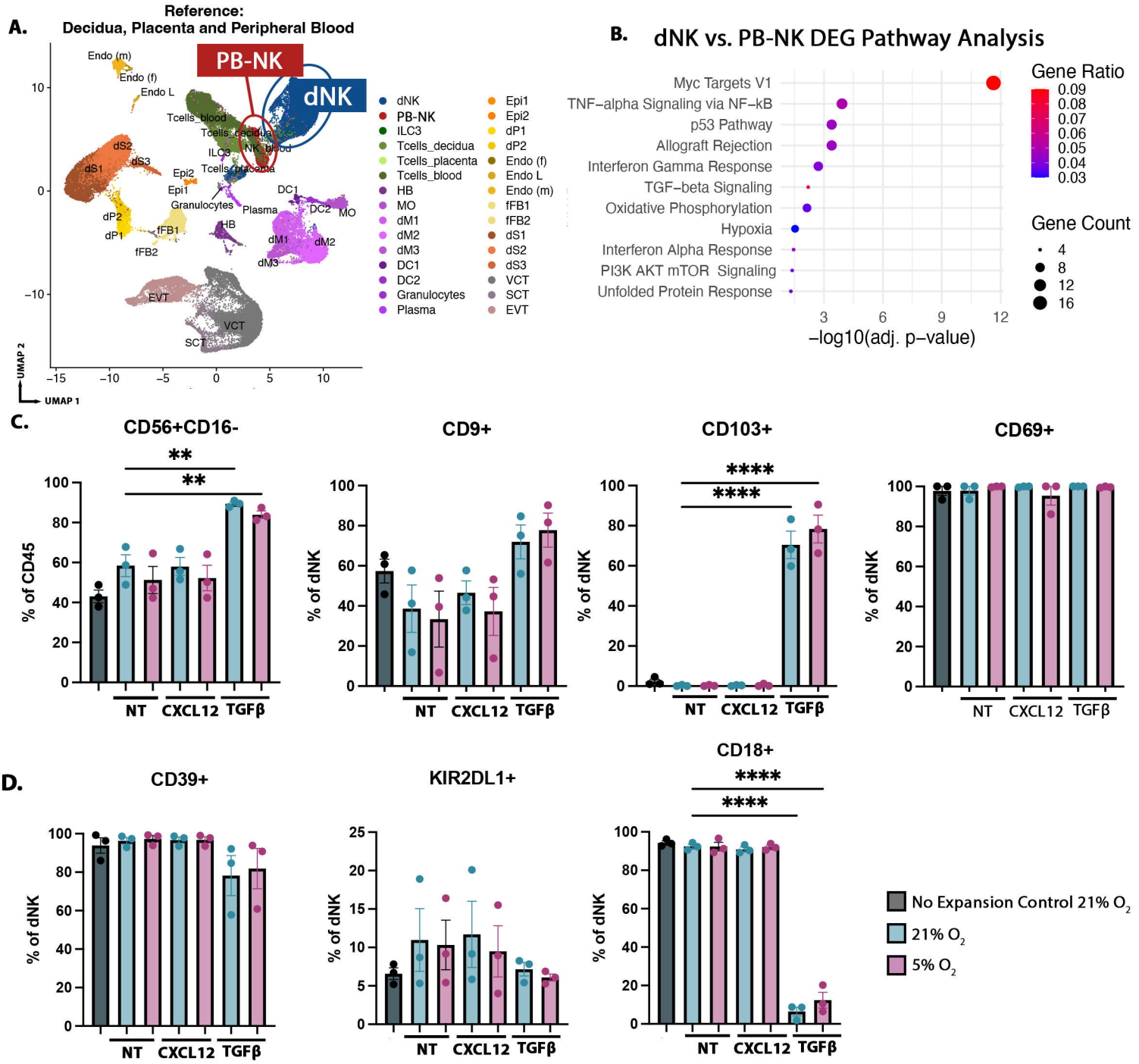
A.
Reference:
Decidua, Placenta and Peripheral Blood
PB-NK
dNK
Endo (m)
Endo (f)
Endo L
Tcells_blood
Tcells_decidua
NK_blood
ILC3
Tcells_placenta
dS2
dS3
dS1
Epi2
Epi1
Granulocytes
Plasma
DC1
DC2
MO
dP2
dP1
fFB1
fFB2
HB
dM1
dM2
dM3
EVT
VCT
SCT
UMAP 2
UMAP 1
dNK
PB-NK
ILC3
Tcells_decidua
Tcells_placenta
Tcells_blood
HB
MO
dM1
dM2
dM3
DC1
DC2
Granulocytes
Plasma
Epi1
Epi2
dP1
dP2
Endo (f)
Endo L
Endo (m)
fFB1
fFB2
dS1
dS2
dS3
VCT
SCT
EVT
B.
dNK vs. PB-NK DEG Pathway Analysis
Myc Targets V1
TNF−alpha Signaling via NF−kB
p53 Pathway
Allograft Rejection
Interferon Gamma Response
TGF−beta Signaling
Oxidative Phosphorylation
Hypoxia
Interferon Alpha Response
PI3K AKT mTOR Signaling
Unfolded Protein Response
−log10(adj. p−value)
Gene Ratio
0.09
0.08
0.07
0.06
0.05
0.04
0.03
Gene Count
4
8
12
16
C.
CD56+CD16-
CD9+
CD103+
CD69+
% of CD45
% of dNK
NT
CXCL12
TGFβ
D.
CD39+
KIR2DL1+
CD18+
No Expansion Control 21% O2
21% O2
5% O2

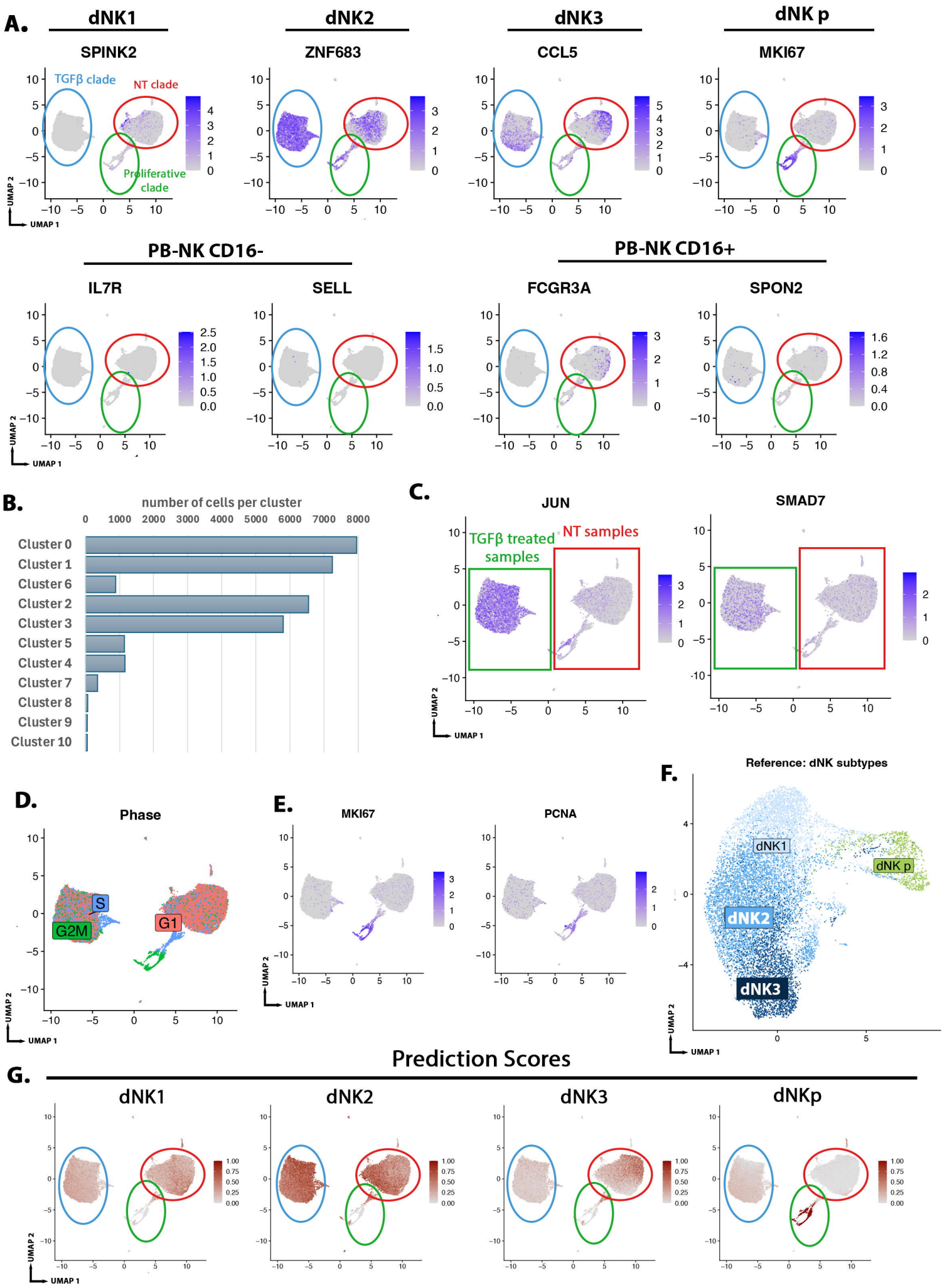
A.
dNK1
dNK2
dNK3
dNK p
SPINK2
ZNF683
CCL5
MKI67
TGFβ clade
NT clade
Proliferative clade
PB-NK CD16-
PB-NK CD16+
IL7R
SELL
FCGR3A
SPON2
UMAP 1
UMAP 2
B.
number of cells per cluster
Cluster 0
Cluster 1
Cluster 6
Cluster 2
Cluster 3
Cluster 5
Cluster 4
Cluster 7
Cluster 8
Cluster 9
Cluster 10
C.
JUN
SMAD7
TGFβ treated samples
NT samples
D.
Phase
S
G2M
G1
E.
MKI67
PCNA
F.
Reference: dNK subtypes
dNK1
dNK p
dNK2
dNK3
G.
Prediction Scores
dNK1
dNK2
dNK3
dNKp

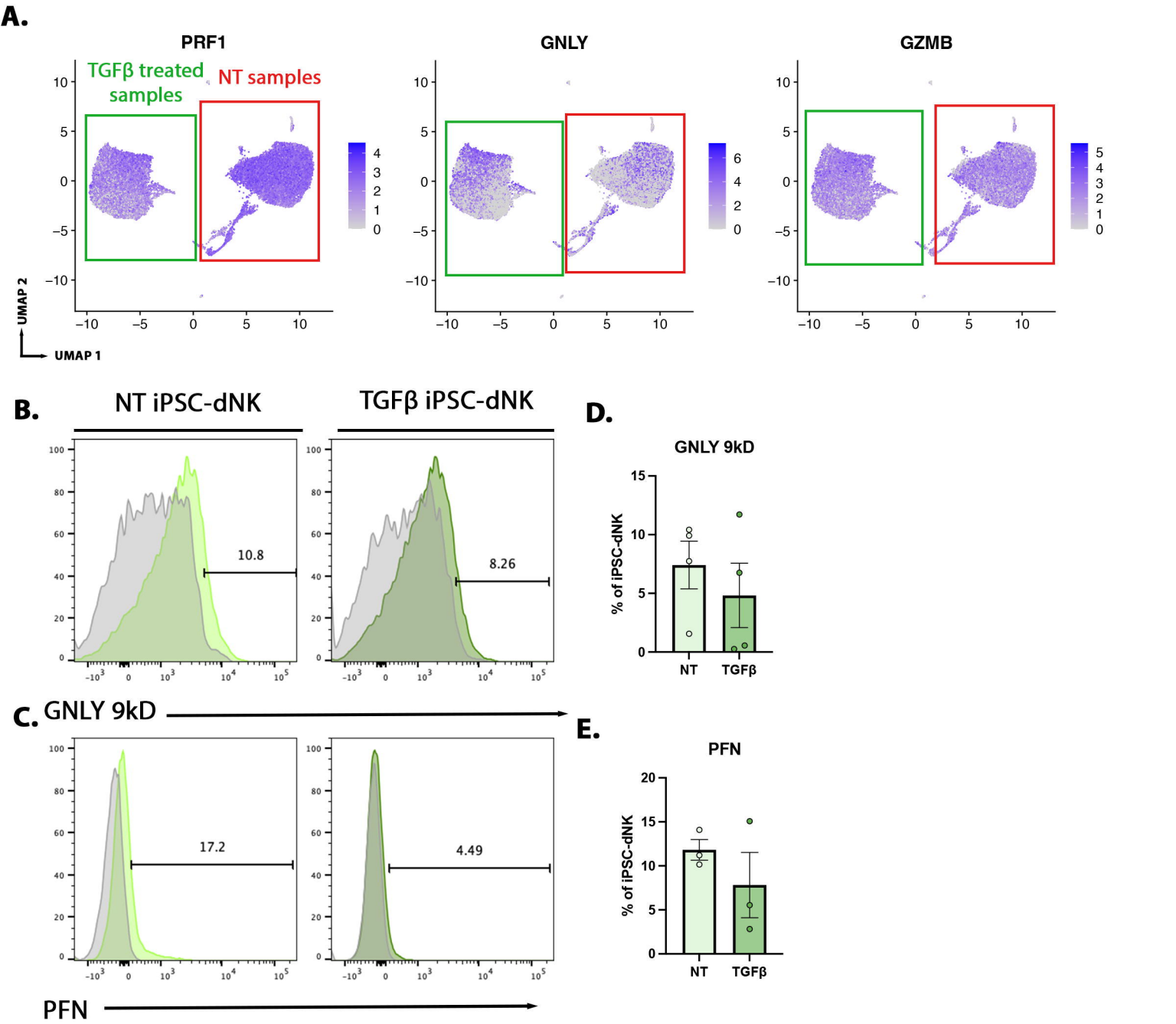
A.
PRF1
GNLY
GZMB
TGFβ treated samples
NT samples
UMAP 2
UMAP 1
B.
NT iPSC-dNK
TGFβ iPSC-dNK
10.8
8.26
C.
GNLY 9kD
17.2
4.49
PFN
D.
GNLY 9kD
% of iPSC-dNK
NT
TGFβ
E.
PFN
% of iPSC-dNK
NT
TGFβ

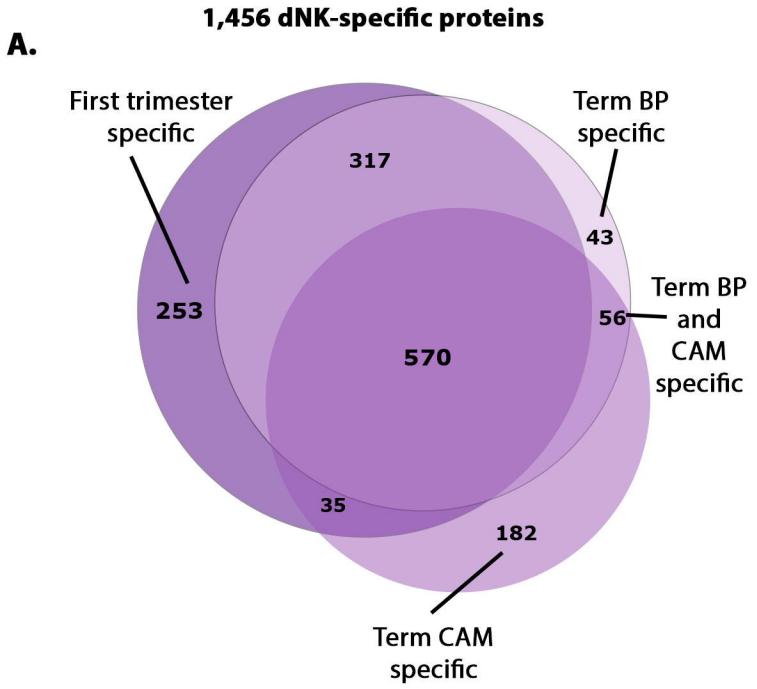
A.
1,456 dNK-specific proteins
First trimester specific
Term BP specific
Term BP and CAM specific
Term CAM specific
317
43
253
56
570
35
182

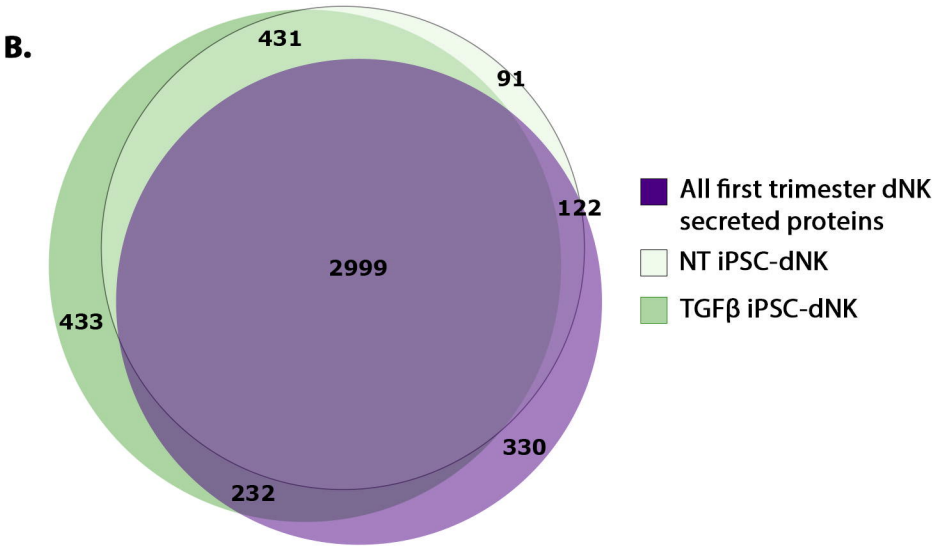
B.
431
91
122
2999
433
330
232
All first trimester dNK secreted proteins
NT iPSC-dNK
TGFβ iPSC-dNK

Table 1. Top 25 marker genes distinguishing dNK cell subtypes (dNK1, dNK2, dNK3, dNKp) and PB-NK cell subtypes (PB-NK CD16^{+}, PB-NK CD16^{-})

dNK1	dNK2	dNK3	dNKp	PB-NK CD16-	PB-NK CD16+
B4GALNT1	*CDHR1*	*ITM2C*	*PBK*	*IL7R*	*FGFBP2*
CYP26A1	*CD2*	*CXCR4*	*CENPA*	*SELL*	*S1PR5*
ENTPD1	*ZNF683*	*TAGAP*	*CDCA3*	*IL18R1*	*AKR1C3*
SPINK2	*COX6A2*	*CD160*	*PLK1*	*IGFBP4*	*SPON2*
TPTEP1	*TNFRSF4*	*LINC01871*	*DLGAP5*	*RIPOR2*	*PRSS23*
C15orf48	*KRT81*	*RGCC*	*KIF23*	*LTB*	*FCGR3A*
EPAS1	*CTSA*	*PDE4B*	*UBE2C*	*PLAC8*	*ADGRG1*
CDKN1A	*IFI44L*	*DUSP4*	*PIMREG*	*TXNIP*	*PLAC8*
CSF1	*C1orf162*	*ARL4A*	*CCNA2*	*LINC00861*	*S100A8*
UBASH3B	*IGFBP1*	*RGS2*	*HMMR*	*RASGRP2*	*LINC00861*
UBE2F	*ITGAX*	*DNAJB1*	*SPC25*	*GZMK*	*TBX21*
DAPK2	*BCO2*	*CEMIP2*	*TOP2A*	*IGKC*	*RIPOR2*
ACY3	*SNRNP25*	*RASGEF1B*	*CEP55*	*TCF7*	*LYAR*
SYNGR1	*KIR2DL4*	*ZNF331*	*RRM2*	*MCUB*	*GNG2*
ID3	*IGFBP2*	*IFRD1*	*AURKB*	*KLF2*	*CD160*
PLPP1	*MATK*	*NFE2L2*	*CKAP2L*	*GRK6*	*TXNIP*
MDM2	*TSPO*	*ZEB2*	*CDCA5*	*KLRF1*	*CLEC2D*
STAT3	*AGTRAP*	*CCNH*	*CDK1*	*SNHG25*	*S100A9*
CD59	*TESC*	*PIK3R1*	*CCNB2*	*LINC01871*	*C1orf21*
SLC12A8	*SLC44A1*	*PTPN22*	*SPC24*	*ITGAM*	*ICAM2*
AFAP1L2	*LASP1*	*PMAIP1*	*KIF2C*	*S100A9*	*TTC38*
PIK3R6	*AHNAK*	*ALOX5AP*	*GTSE1*	*TRGC2*	*FAM107B*
CAMK1	*SEPTIN11*	*TIPARP*	*CDCA8*	*ATM*	*C12orf75*
BCL2L11	*GZMH*	*SERTAD1*	*NUSAP1*	*ARHGAP15*	*LBH*
SRGAP3	*CHCHD10*	*ITGAE*	*BIRC5*	*VPS51*	*PPP2R5C*